

# We are IntechOpen, the world's leading publisher of Open Access books Built by scientists, for scientists

6,900

Open access books available

185,000

International authors and editors

200M

Downloads

Our authors are among the

154

Countries delivered to

TOP 1%

most cited scientists

12.2%

Contributors from top 500 universities



WEB OF SCIENCE™

Selection of our books indexed in the Book Citation Index  
in Web of Science™ Core Collection (BKCI)

Interested in publishing with us?  
Contact [book.department@intechopen.com](mailto:book.department@intechopen.com)

Numbers displayed above are based on latest data collected.  
For more information visit [www.intechopen.com](http://www.intechopen.com)



---

# Titanium Dioxide Modifications for Energy Conversion: Learnings from Dye-Sensitized Solar Cells

---

Hammad Cheema and Khurram S. Joya

Additional information is available at the end of the chapter

<http://dx.doi.org/10.5772/intechopen.74565>

---

## Abstract

During the last two and half decade modifying anatase  $\text{TiO}_2$  has appreciably enhanced our understanding and application of this semiconducting, non-toxic material. In the domain of DSCs, the main focus has been to achieve band adjustment to facilitate electron injection from anchored dyes, and high electronic mobility for photo-generated electron collection. In retrospection, there is a dire need to assimilate and summarize the findings of these studies to further catalyze the research, better understanding and comparison of the structure–property relationships in modifying  $\text{TiO}_2$  efficiently for crucial photo-catalytic, electrochemical and nanostructured applications. This chapter aims at categorizing the typical approaches used to modify  $\text{TiO}_2$  in the domain of DSCs such as through  $\text{TiO}_2$  paste additives,  $\text{TiO}_2$  doping, metal oxides inclusion, dye solution co-adsorbing additives, post staining surface treatment additives and electrolyte additives. A summary of the consequences of these modifications on electron injection, charge extraction, electronic mobility, conduction band shift and surface states has been presented. This chapter is expected to hugely benefit the researchers employing  $\text{TiO}_2$  in energy, catalysis and battery applications.

**Keywords:** modification, co-adsorption, surface treatment, recombination, electron lifetime, electronic mobility, photovoltage

---

## 1. Introduction

Global energy demand is expected to increase from 18 TW in 2013 to 50 TW in 2050, along with corresponding increase in  $\text{CO}_2$  emissions due to inevitable increase in population and industrialization in the developing world [1, 2]. So far, most of the energy (~80%) have been derived from fossil fuels, which is not sustainable and detrimental to the environment [2]. Thus,

sustainable and fossil-free pathways for producing clean energy and fuels such as conversion of sunlight to electricity and molecules in atmosphere, e.g., water, CO<sub>2</sub> and nitrogen, to H<sub>2</sub>, hydrocarbons and ammonia respectively are highly required [3–8]. In this regard, dependence on renewable energy sources such as solar, wind and hydroelectric has been strategically deployed from last few decades with reasonable effect [5, 7]. Among all the renewable energy sources, solar energy is the most potent and exploitable source [9]. However, in order to achieve large scale, cost effective, carbon neutral supply of energy from sun; capture, conversion and storage of energy should be highly efficient and cost effective [6, 9]. In this regard, photovoltaics (PVs) are playing a substantial role in harnessing the sun energy mainly dominated by silicon based solar cells at present. However, manufacturing of silicon PVs require high temperature (>1600°C for silicon melting) and ultra-pure materials, thus adding to the manufacturing complexity and cost [10]. Additionally, the scarcity of silver, a common electrode material greatly limits to meet the future terawatt challenge. This have motivated researchers around the globe to develop strategies for solar energy conversion based on abundant, non-toxic, easy to process, commercially viable and cost effective systems. In this regard solar PVs prepared from mesoscopic metal oxides such as (TiO<sub>2</sub>, ZnO, SnO<sub>2</sub>, etc.) and organic light absorbing materials could meet the criteria as a suitable alternative, provided high efficiency can be realized. Metal oxide serves as an electron acceptor and facilitates the transport of electrons, along with being a scaffold for the adsorption of light harvesting constituents in many cases [11, 12]. Out of different metal oxides, mesoscopic (10–50 nm size pores) titanium dioxide (TiO<sub>2</sub>) by far has been the most widely studied and employed owing to ease process-ability, chemical stability, high surface area, low cost and non-toxic nature. [12–15] Out of the four naturally occurring polymorphs of TiO<sub>2</sub>, anatase (tetragonal), rutile (tetragonal), brookite (orthorhombic), and TiO<sub>2</sub> (monoclinic), anatase is preferred for PV's applications because of higher conduction band energy and slower recombination rate of charge carriers [16–18].

In terms of mesoscopic-TiO<sub>2</sub> based solar cells, dye-sensitized solar cells (DSCs) are the most widely studied with recent surge in research for perovskite solar cells [12, 19, 20]. The discussion in the remaining chapter will be with the reference to DSCs employing TiO<sub>2</sub> as electron accepting and transport layer. The seminal report of 1991 on TiO<sub>2</sub> based DSCs by Grätzel and O' Regan has garnered more than 26,500 citations (November 2017) highlighting the plethora of knowledge generated and wide spread interest of scientific community [11]. It should be noted that nanocrystalline morphology which goes through necking as the result of sintering and lead to mesoscopic film of TiO<sub>2</sub> is essential for the efficient operation of the DSCs, since a monolayer of sensitizer on flat metal oxide surface only absorb small portion of incident light [13]. Realization of this important nanostructure requirement aspect enhanced the adsorption and subsequent light harvesting in DSCs by molecular sensitizers or dyes more than 1000 time [13]. This enabled DSCs only system where charge generation (sensitizer) and transport (semiconductor) is performed by separate components. [14] DSCs are attractive compared to other photovoltaic technologies in terms of economic advantage, tunability of color, can be built on rigid and flexible substrates, made of benign materials such as TiO<sub>2</sub> and metal free organic dyes, offer sustained efficiency for indoor applications, and perform independently of the angle of incidence [11, 12, 21–24]. Current, DSC record power conversion efficiency (PCE) up

to 14.3% has been demonstrated by judicious choice of co-sensitizing organic photosensitizers having strong binding to  $\text{TiO}_2$  and broad absorption, post staining surface capping and tailored solution based redox shuttle and electrolyte additives [25]. However, for further improvement in PCE (1) sensitizers with efficient conversion of absorbed photons to electrons (400–900 nm), particularly beyond 650 nm (2) redox shuttles with photovoltage output greater than 1.2 V (3) minimized recombinations and over potential losses and (4) optimized tandem devices are highly required [26–29].

The standard components of a typical DSC embodiment are (1) FTO (fluorine doped tin oxide) deposited on glass substrate (2) mesoscopic  $\text{TiO}_2$  film (3) sensitizer, organic or metal complex anchored to  $\text{TiO}_2$  (4) mediator, to regenerate the dye (5) counter electrode with platinum (pt) to reduce the mediator (**Figure 1**). Upon illumination the sensitizer gets photo-excited and injects an electron in the conduction band (CB) of  $\text{TiO}_2$  thus generating an electric potential difference. This injected electron then diffuses through the mesoporous  $\text{TiO}_2$  where it is extracted to outer circuit at photoanode. Meanwhile the oxidized sensitizer is regenerated by the redox mediator, whereas the extracted electron travels through the load to the counter electrode, which then transfers electron to the mediator. At the interface boundary, back electron transfer to the oxidized dye and recombination with the electrolyte has been known the most drastic events which lower the performance along with inefficient light absorption beyond 650 nm [13, 14]. On the same note before printing the mesoporous  $\text{TiO}_2$  film a compact  $\text{TiO}_2$  layer (mostly from aqueous  $\text{TiCl}_4$  solution) is deposited on the FTO glass which prevents the short circuiting of the device, improves adhesion of  $\text{TiO}_2$  nanoparticles and minimizes the direct contact of electrolyte with FTO [30–32]. In terms of characterization of DSCs, two important measurements are short photocurrent-density ( $J_{sc}$ ) and open circuit voltage ( $V_{oc}$ ) curve also known as

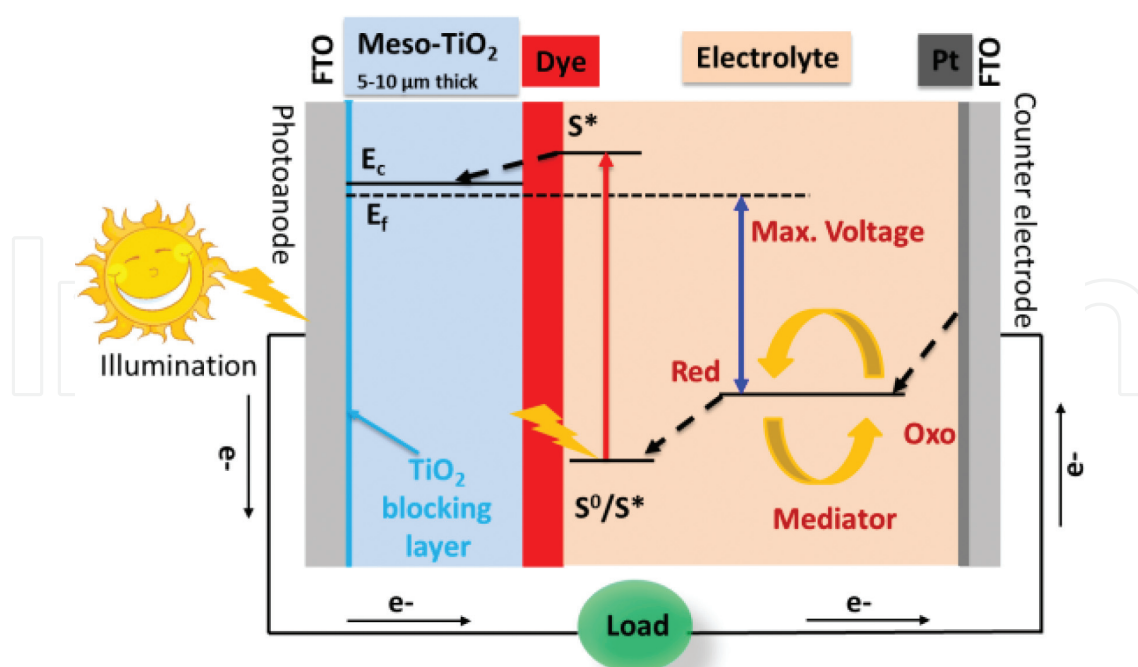


**Figure 1.** Operational principle of DSCs.

$J$ - $V$  curve and incident photon to current conversion efficiency (IPCE) or EQE (external quantum efficiency). IPCE depicts the photocurrent density response of the device at monochromatic wavelength and depends on the same parameters as  $J_{sc}$  [33].

$J$ - $V$  curve is measured by scanning the voltage across the device from 0 to higher voltage (forward bias) or higher to zero voltage (reverse bias) either with a source meter or a potentiostat. Power conversion efficiency (PCE) of the cells, the main performance metric is then calculated according to the equation,  $PCE = (J_{sc} V_{oc} FF)/I_0$ , where  $FF$  is the fill factor which is simply the measure of the squareness of the  $J$ - $V$  curve, and depicts the electrochemical losses in the device with value between 0 and 1 (normally between 0.65 and 0.75 for DSCs) [34].  $I_0$  is the power input for the incident irradiation which is normally 1 sun ( $100 \text{ mW/cm}^2$ ). A high performing DSC should behave an ideal diode with infinite shunt resistance and minimum series resistance which will lead to higher  $FF$  and PCE ultimately [13]. Briefly,  $J_{sc} \propto \text{LHE} \cdot \phi_{inj} \cdot \phi_{reg} \cdot \eta_{coll}$ , where LHE is light harvesting efficiency of sensitizer on given thickness of  $\text{TiO}_2$ ,  $\phi_{inj}$  and  $\phi_{reg}$  are the quantum yield of electron injection and dye regeneration and  $\eta_{coll}$  is the charge collection efficiency [12].

In **Figure 2**, thermodynamic requirements for electron injection (up to 300 mV) and dye regeneration (100–500 mV) overpotential has been shown. Dotted lines highlight the unwanted recombination reactions with redox shuttle ( $10^{-2}$  sec) and oxidized sensitizer ( $10^{-4}$  sec) also known as “dark current” [12, 35, 36]. Kinetically, electron injection happens in 100 s of pico seconds and vary with sensitizer, with usual ms to  $\mu\text{s}$  range of recombination with electrolyte and oxidized dye, respectively. [24] Tuning of electrochemical properties of sensitizers (Ru (II), organic, and porphyrin) with optimized geometry offering higher light absorption and minimum aggregation and redox shuttles (iodide/triiodide, cobalt and copper) has been widely studied for DSCs with the aim of minimum overpotential loss, broad absorption and higher PCE [37–40]. Interested readers are encouraged to consult the more detailed reviews on design principles of sensitizers and redox shuttles for DSCs [21, 33, 40–43].

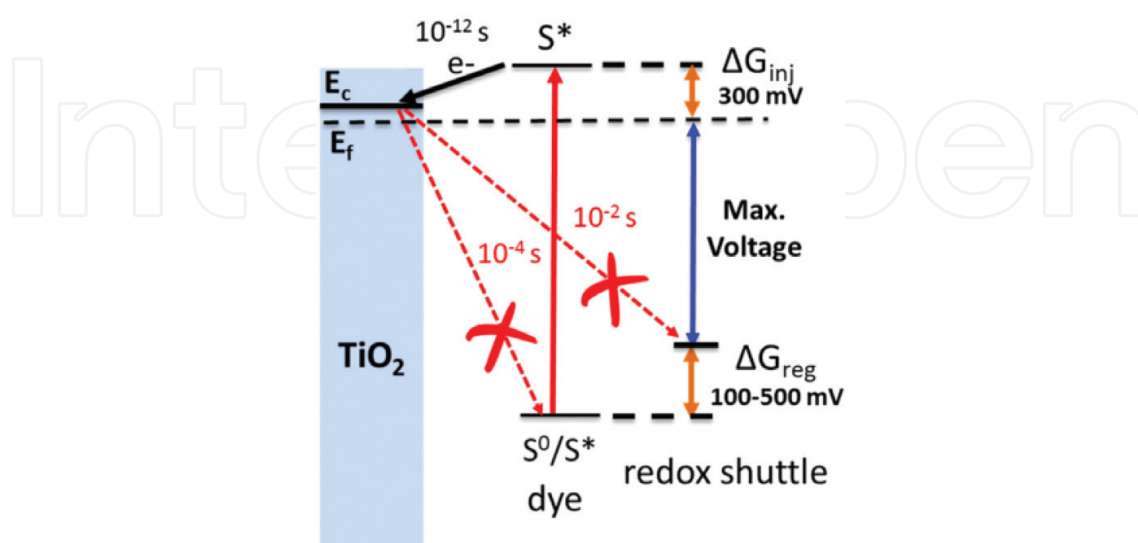


**Figure 2.** Energy level diagram, overpotential requirements and typical time constants.



$J_{sc}$  can be increased by molecular engineering of the sensitizer, with ideal ground and excited state energetics, high molar absorptivity, and aggregation less anchoring on  $\text{TiO}_2$  [12].  $V_{oc}$  is the energy difference between the  $\text{TiO}_2$  fermi level and the redox potential of the mediator and depends on the electron density in  $\text{TiO}_2$ . Higher  $V_{oc}$  can be achieved by minimization of the dark current, increase in electron injection, negative (upward) shift in the energy of the conduction band, positive (downward) shift in the energy of the redox shuttle and series connection of devices [35, 44]. Both  $V_{oc}$  and  $FF$  are hugely related to recombination reactions (dark current) and can be substantially influenced by modification of  $\text{TiO}_2$  in the presence of additives *vide infra*. Along with  $J$ - $V$  and IPCE measurements, electrochemical impedance spectroscopy (EIS) and small modulation photovoltage transient measurements have been widely employed to fully characterize the devices. Readers are kindly referred to the previously published reviews to learn about these powerful techniques to characterize interface and charge transfer properties [45–48].

In terms of achieving higher efficiency by modification of  $\text{TiO}_2$  the main objective is to minimize the recombination losses by blocking the  $\text{TiO}_2$  surface, increase in electron injection by manipulation of  $\text{TiO}_2$  CB, aid in better orientation, structure and geometry of the dyes on  $\text{TiO}_2$  and suppression of dye aggregation and stacking. This enhancement of DSCs devoid of dye and electrolyte designing and arduous manipulations of their molecular structures can be achieved by (1)  $\text{TiO}_2$  paste additions (2) dye solution co-adsorbing additives (3) post staining surface treatment additives and (4) electrolyte additives (**Figure 3**). This chapter is now further divided into sections as shown in **Figure 3**. to integrate and analyze the most successful strategies, their role in enhancing DSCs performance, similarities among different approaches and discussion of proposed mechanisms.

It is crucial to highlight that just like dyes for DSCs most of the additives will require an anchoring group for immobilization on  $\text{TiO}_2$ , other than plasmonic nanoparticles and composite of  $\text{TiO}_2$  NPs (Section 1, which become the intrinsic part of  $\text{TiO}_2$  NPs after sintering also termed as “hard modification”). The most widely used anchoring groups are same as dyes, e.g., carboxylic acid, phosphonic/phosphinic acid, pyridine, and most recently siloxanes. Though multitude of anchoring modes such as covalent attachment, hydrogen bonding, electrostatic interaction, van der Waals interaction and physical entrapment has been proposed [49]. It is important to notice that these anchoring systems should also facilitate the electron transfer. Additionally, due to structural complexity of the interface environment several models are used to elucidate the anchoring. For physical characterization of interface Fourier

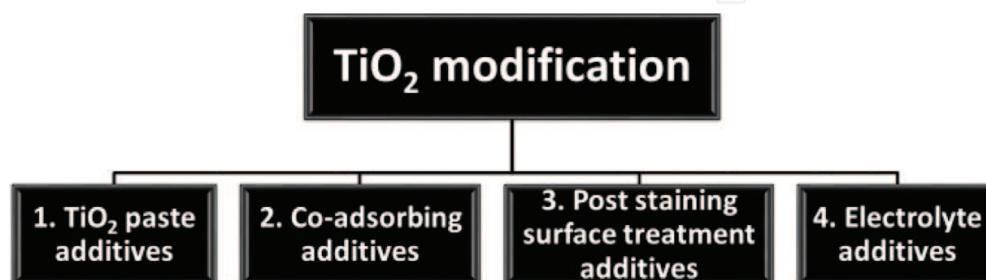


**Figure 3.** Summary layout for  $\text{TiO}_2$  modification approaches.

transform infrared spectroscopy (FT-IR) and photoelectron spectroscopy (PES) are mainly employed [50]. However for anchoring on  $\text{TiO}_2$  for the well-known carboxylic acid, (similarly anchoring phosphonic/phosphinic acid, siloxane, etc.) (Figure 4) covalent interaction can only offer the strongest coupling for stable anchoring with ester type bonds or metal complexation for pyridine additives [51]. For an in depth analysis of anchoring mode and surface adsorption for different anchoring groups, readers are kindly referred to reviews published previously [49, 51].

For efficient light harvesting different kinds of  $\text{TiO}_2$  pastes (active layer for dye anchoring with scattering or reflective layer on top of it) are used for achieving specific features such as iodide/triiodide systems mainly employ 18–20 nm size NPs based formulations, whereas for larger size redox shuttles such as cobalt and copper based systems 28–31 nm size NPs are employed [52, 53]. This selectivity comes from the mass-transport related limitations of outer sphere based redox shuttles (cobalt and copper) which is mitigated by the larger pore size of bigger NP size based  $\text{TiO}_2$  films [54]. On top of active layer, 4–5  $\mu\text{m}$  thick scattering or reflective layer is printing with NPs size of >100 nm, to back scatter light into the cell.

### 1.1. Scope

Though synthesis and preparation of  $\text{TiO}_2$  paste for film formation has historical importance, however, at this stage more than 95% of the studies employ a commercially available  $\text{TiO}_2$  paste which is developed after years of research and employ patented methods [53, 55]. However, design of morphologically new structures, and development of efficient synthesis routes for anatase  $\text{TiO}_2$  is an active area to achieve higher loading, better charge transport, and minimum recombinations losses [18]. For this chapter please be referred to commercially available  $\text{TiO}_2$  (transparent 18–20 nm from Dyesol or Solaronix, or 30–31 nm from Dyesol or Dyenamo nm particle size for active layer and > 100 nm size for scattering layer from Dyesol, Solaronix and Dyenamo) for improvement [56–58]. With ready to use  $\text{TiO}_2$  paste in hand, its light absorption properties can be enhanced by simple mixing in systematic way with silver

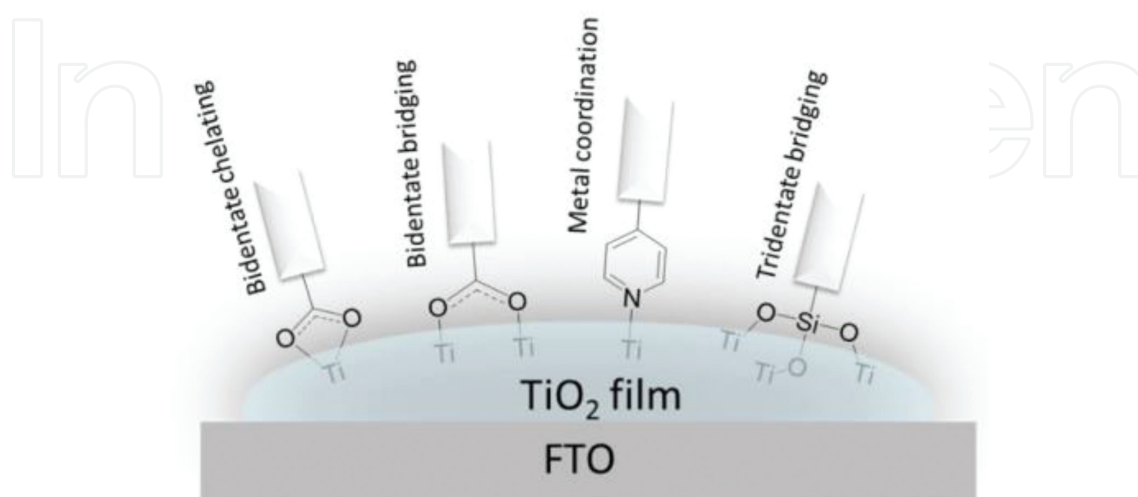


**Figure 4.** Depiction of anchoring mode of general additives for  $\text{TiO}_2$  modifications.

and gold nanoparticles (Section 1). Additionally, different types of  $\text{TiO}_2$  geometries such as nanotubes (NTs) and hollow spheres can be mixed with nanoparticles (NPs) to achieve higher loading (Section 1.2 and 1.3). An important class of additives to modify and enhance the interface properties of  $\text{TiO}_2$  is the addition of electronically insulating molecules with anchoring groups (Section 2). Quite recently, simple surface treatment by chemical bath method on dye anchored  $\text{TiO}_2$  (stained) films has been explored with impressive enhancements, such strategies are discussed in Section 3. Historically, most widely studied approach in regard to enhancement of DSCs and modification of  $\text{TiO}_2$  is the introduction of new electrolyte additives including solvent, surface and recombination blocking pyridines and different anchoring groups, which are discussed in Section 4. At the end an overall perspective on the state of DSCs and the role of learnings to other fields is analyzed.

## 2. $\text{TiO}_2$ paste modifications

Integration of subwavelength plasmonic nanostructures and morphologically varied mesoporous films of  $\text{TiO}_2$  have been widely explored for enhancing DSCs performance. Hard modification of  $\text{TiO}_2$ , such as sintering step is required at high temperature (500 °C) to activate the functionality are discussed below.

### 2.1. Plasmonic enhancement of DSCs

Plasmonic enhancement or light entrapment in DSCs by means of the plasmonic resonance of metal nanostructures has been a topic of intense research in the last decade. Since the first report in 2000 of metal nanostructured mediated enhancements in DSCs, many successful studies has been published outlining the role of size, shape and composition of metal nanoparticles on DSCs performance and working mechanisms [59–61]. Metal nanostructures capable of surface plasmon such as Au and Ag has been systematically introduced with  $\text{TiO}_2$  NPs. Such as these nanoparticles can be designed and integrated in  $\text{TiO}_2$  NPs in a way to offer light entrapment from visible to NIR region [62].

In plasmonic materials the coupling of incident photons to conduction band electrons upon excitation give rise to collective oscillations of electrons defined as *localized surface plasmon resonances* (LSPR) [63, 64]. By the engineering of plasmonic nanostructure's geometry, dimensions and composition LSPR's radiative (hot electron transfer, plasmon resonant energy transfer) and non-radiative (far-field scattering >50 nm size, near field coupling 3–50 nm size) processes can be tailored (**Figure 5**) [55, 56]. Out of four processes summarized in **Figure 5** far-field scattering and near field coupling are easily observed for DSCs such as by improvement in IPCE, whereas role of hot electron transfer and PRET to improve DSCs is thus far poorly explored [62]. Detailed discussion of each process and its implications for DSCs are beyond the scope of this chapter [62, 65].

In radiative effects metal nanostructure acts as a secondary light source and in non-radiative effects absorbed energy is subsequently transferred to neighboring semiconductor NPs (**Figure 5**).



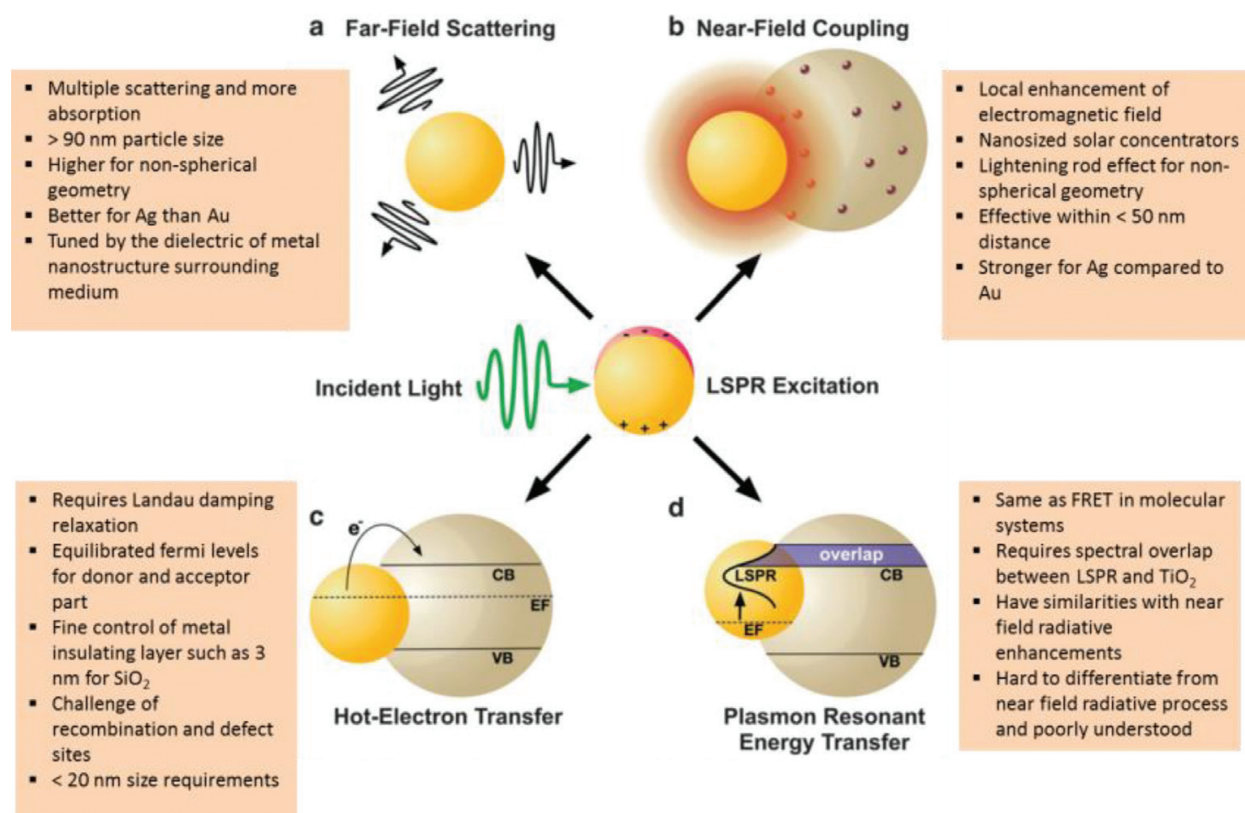


**Figure 5.** Summary of radiative (a) and (b) and non-radiative LSPR-based processes and their features, modified from reference [62], with permission from the Royal Society of Chemistry.

For LSPR based enhancement of DSCs the size of the metal nanoparticles plays huge role. Such as at 5 nm regime of metal nanostructure non-radiative processes are dominant, near field coupling for 45 nm size regime and far field scattering for 120 nm size metal nanostructures [62]. In terms of application, some reports evidence the beneficial effect of topical presence of plasmonic nanoparticles on  $\text{TiO}_2$  film, however, homogenous integration of plasmonic nanoparticles throughout active layer have proven more efficient, particularly in enhancing photocurrent response of devices (**Figure 6**) [67, 68].

The highest PCE achieved through plasmonic enhancements so far (2013) is 10.8% which is 30% higher (8.3% PCE) than the control device employing **N719** sensitizer by Belcher et al. with 0.01–0.32% core shell particles mixed with regular  $\text{TiO}_2$  [61]. In this study, oxide-metal-oxide multiple core-shell nanostructured spheres were blended with already available photoactive materials to achieve balanced light harvesting in panchromatic fashion. Kamat et al. in a pioneering work (2012) identified the plasmonic and charging effect based on the composition of  $\text{Au@SiO}_2$  and  $\text{Au@TiO}_2$ , leading to achieve a higher photocurrent and photovoltage with overall PCE of 10.2 and 9.7%, respectively [60]. Au nanoparticles of 5 nm size were used in the core with shell as passivation layer of either  $\text{SiO}_2$  or  $\text{TiO}_2$  and mixed with Solaronix T/SP paste in 0.7 wt%. Wang et al in 2013, in a unique study employed the organic sensitizer **FNE29** and  $\text{I}^-/\text{I}_3^-$ , along with  $\text{TiO}_2$  inlaid 2 nm sized Au nanoparticles resulting in 10.1% PCE improved from 5.5% PCE (84% increase) [66]. Au nano colloid in 0–0.8 wt% ratio

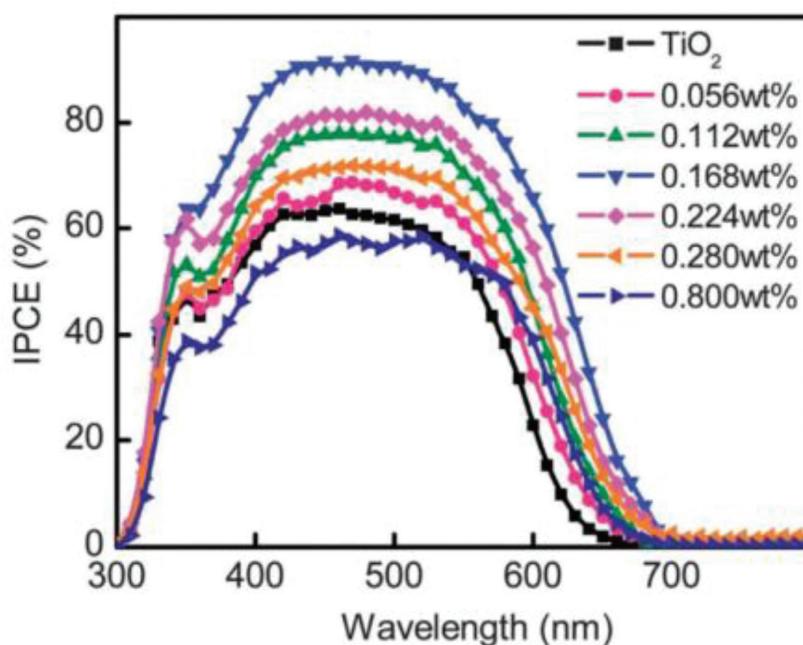


**Figure 6.** Effect of ~2 nm sized inlaid Au NPs with different wt% in TiO<sub>2</sub> paste on IPCE, adopted from Ref. [66], with permission from the Royal Society of Chemistry.

was blended with TiO<sub>2</sub> paste to constitute the active layer (**Figure 6**). With most prominent current report, DSCs employing organic dye (**FNE29**) compared to Ru (II) dyes for plasmonic enhanced DSCs are rare. With the survey of reports published so far it is clear that though plasmonics has led to increased device efficiencies however, reports lack (1) application of non-precious metal plasmonics for enhanced DSCs such as Al, graphene and semiconducting nanocrystal plasmonics (2) application of metal nanoparticles in conjunction with high photovoltage redox shuttles such as Co (III/II) or Cu (II/I) and organic sensitizers (3) long term stability studies particularly against redox shuttles for corrosion and chemical resistance of plasmonic DSCs [69–74].

## 2.2. Morphological investigation on TiO<sub>2</sub>

NP based mesoporous TiO<sub>2</sub> shows excellent features for DSCs however it suffers from low electrical conductivity and charge recombination losses [75–78]. Additionally, enhanced light scattering and dye adsorption can be achieved by modifying the shape of NPs or mixing nanotubes, nanowires, nanospheres, and hollow TiO<sub>2</sub> [58, 77–81]. On the same note, 2D and 3D structures of TiO<sub>2</sub> such as nanoribbons, nanodisks, nanoleaves, nanoflowers, nanorods, hedgehog nanostructure and dendritic hollow structures have also be explored for DSCs [82–87]. The studies focused on the morphological modification of TiO<sub>2</sub> have demonstrated marginal increase in DSC performance with scattered results, however, due to structural complexity and reproducibility issues such investigations has not resulted in wide spread application for DSCs [76]. For details please refer to the cited work.

### 2.3. Metals and metal oxides for TiO<sub>2</sub> modifications

Doping or intentional addition of impurities while synthesis of TiO<sub>2</sub> can have substantial effect on band structure and surface states which dictate charge transport and dye/TiO<sub>2</sub> interface in DSCs [88]. The purpose of doping is to achieve higher conductivity and minimized recombinations. In the regime of DSCs, doping has been studied with metals (lithium, magnesium or calcium), metalloids (boron, silicon, germanium, antimony), non-metals (carbon, nitrogen, sulfur, fluorine and iodine), transition metals, post transition metals and lanthanides. For a detailed analysis on choosing the dopant and its effects interested readers are referred to previously published review on the topic [88]. These dopants are generally added during the synthesis stage and require subsequent sintering step to be integrated as the part of crystalline structure of TiO<sub>2</sub> (hard modification).

Additionally, to enhance the interface properties of DSCs at TiO<sub>2</sub>/dye/electrolyte for efficient charge transfer wide bandgap and electronically insulating metal oxides has been widely studied [75, 89]. Wide band gap metal oxides such as ZnO, Nb<sub>2</sub>O<sub>5</sub>, and WO<sub>3</sub> and electronically insulating oxides such as SrO, Al<sub>2</sub>O<sub>3</sub>, ZrO<sub>2</sub> and SiO<sub>2</sub> are known to form barrier layer at the interface which impedes back electron transfer at the interface boundary thus lowering recombination losses [90]. Most recently, MgO have been studied for TiO<sub>2</sub> modification during synthesis, leading to negative shift of up to 200 mV of TiO<sub>2</sub> owing to its more basic nature [91, 92]. An alternative approach is to surface treat the TiO<sub>2</sub> film with Mg<sup>+2</sup> precursor such as (Mg (OC<sub>2</sub>H<sub>5</sub>) or Mg (NO<sub>3</sub>)<sub>2</sub>) followed by high temperature sintering, however, concentration control becomes very critical for final performance [90, 93, 94]. Albeit, these studies report higher  $V_{oc}$  for DSCs employing Mg<sup>+2</sup> and reduced recombination losses. However, negatively shifted conduction band can also lower the electron injection if the sensitizer-excited state potential gets very close to CB energy. Interested readers are referred to relevant reviews for in-depth analysis of such modifications [75, 89].

### 3. Dye solution co-adsorbing additives

“Soft modification,” simple rinse and dry to alter TiO<sub>2</sub>/dye/electrolyte interface favorably is to add additives along with the dye adsorption solution known as “co-adsorbents” [95–98]. These additives are also known as de-aggregating agents which aid in favorable dye orientation on TiO<sub>2</sub> and increased electron injection through minimization of dye–dye intermolecular charge transfer and  $\pi$ - $\pi$  stacking [99]. These mainly insulating additives are known to occupy the vacant spaces among dye molecules which prevents the diffusion of oxidized redox species (e.g., I<sub>3</sub><sup>−</sup>) to TiO<sub>2</sub> (**Figure 7**) [100, 101]. This approach has been widely explored for DSCs since the first report in 1993, though such modifications of TiO<sub>2</sub> surface were already explored by Miyasak et al. in 1978 [95, 96]. These co-adsorbents are amphiphilic in nature and consists of an anchoring group (**Figure 4**) such as carboxylic or phosphonic/phosphinic moiety and a long alkyl chain or three dimensional aromatic and alkyl components acting as a buffer between TiO<sub>2</sub> and electrolyte. These co-additives can be divided based on the chemical identity of anchoring group and their influence on the interface can be best studied through EIS and

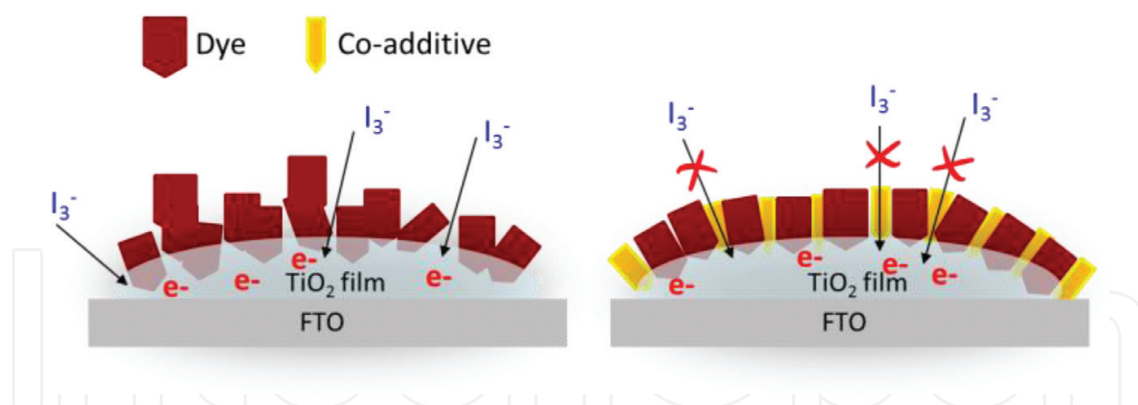


**Figure 7.** Illustration of dye on  $\text{TiO}_2$  surface with (right) and without co-additive,  $\text{I}_3^-$  is the oxidized redox component.

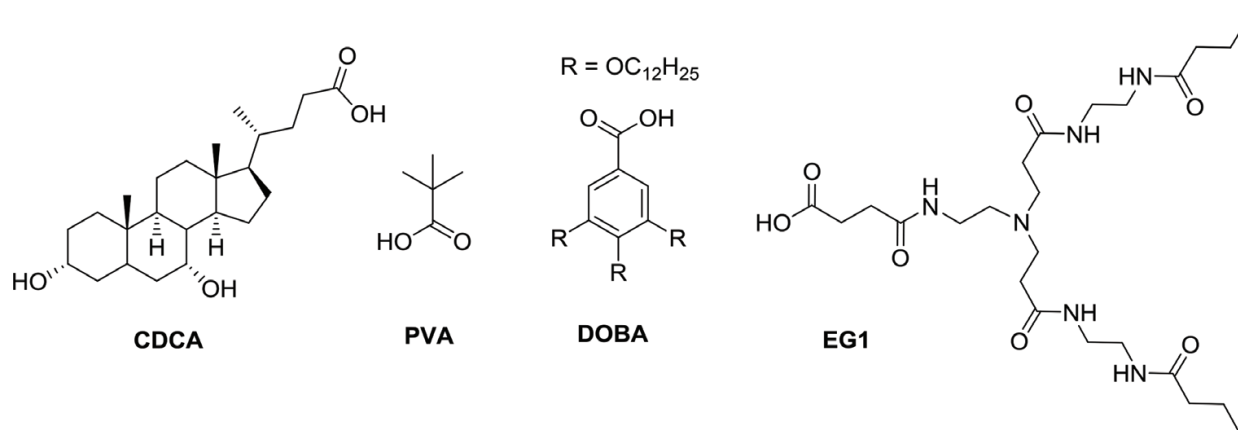


**Figure 8.** Representative co-additives.

electron lifetime measurements. Since aggregation is a common phenomenon for mostly planar organic sensitizer including phthalocyanine and porphyrin, the effect of co-additives on aggregation can be studied by simple current dynamic measurements at different light intensities [102, 103].

### 3.1. Carboxylic acid based anchoring co-additives

Since the first report on deoxycholic acid (DCA) and chenodeoxycholic acid (CDCA, **Figure 8**) in 1993 by Grätzel et al. in ethanolic dye solution along with the sensitizers, CDCA has become the most widely used co-additive [96]. CDCA adsorption for pre-stained and post stained  $\text{TiO}_2$  films was found less effective in terms of enhancing  $J_{sc}$  and  $V_{oc}$  [104]. Generally, the optimum concentration of CDCA in the dye solution depends on the nature of the dye and study of several concentrations (such as 2, 10, 20, and 40 times, etc., of the dye) is a normal routine [105, 106]. It should be kept in mind that excess of CDCA or any other co-adsorbent can adversely affect the dye loading as well. Under optimum conditions, CDCA is generally known to positively (downward) shift the conduction band of  $\text{TiO}_2$ , increasing electron injection along with lower recombination losses thus enhancing both  $J_{sc}$  and  $V_{oc}$ . It should be noted that CDCA mainly serves the role of de-aggregating agent for organic, porphyrin and phthalocyanine



sensitizers and a recombination blocking agent for Ru (II) sensitizers since latter dyes do not aggregate on  $\text{TiO}_2$  [102]. In a recent study for ladder-like carbazole donor and cyanoacrylic acid (CA) anchor based D-A- $\pi$ -A type dye, CDCA resulted in up to 9% enhancement in PCE when co-adsorbed with the dye [107]. Concentration of CDCA was 5 mM compared to 0.3 mM of the dye. The effect for the presence of CDCA was analyzed through EIS measurements which confirmed higher recombination resistance leading to 8% increase in  $J_{sc}$  and 2% increase in  $V_{oc}$  for most efficient dye in the series (**C1**). In a similar study for an organic phenothiazine based dye (**P2**), effect of different concentrations of CDCA was studied in detail [106]. CDCA concentration of 10 mM was found to result in optimum improvement in DSCs performance compared to 0.3 mM concentration of the dye.

**Figure 8** shows the CDCA alternatives such as pivalic acid (PVA), 3,4,5-Tris(dodecyloxy) benzoic acid (DOBA) and EG1 (an amidoamine dendritic molecule) [108–110]. PVA in a comparative study approach showed enhanced electron lifetime and negative shift in the conduction band of  $\text{TiO}_2$ . This lead to 53 mV increase in  $V_{oc}$  and 8% increase in PCE. Adsorption of PVA before staining was found to be more effective, compared to co-adsorption with the dye. In an example with ss-DSCs (solid state-DSCs), DOBA and **Z907** sensitizer resulted in negative shift of the  $\text{TiO}_2$  CB, decreased charge recombination, higher hydrophilicity and enhanced PCE as evidenced by EIS, and IMVS (intensity modulated photovoltage decay spectroscopy) measurements. In another example, strategically designed amidoamine-dendron based molecules (EG0–2) were studied as the co-additives and compared with CDCA. This study showed that superior surface blocking, higher electron injection, minimized intermolecular energy transfer and higher PCE can be tailored with increasing size of the dendritic molecules. In spite of co-additives examples (**Figure 8**), CDCA is mostly widely employed co-additive to modify the interface on  $\text{TiO}_2$ , however, it should be employed with caution particularly in terms of its co-adsorbing concentration.

### 3.2. Phosphonic/phosphinic acid anchoring and zwitterion-based co-additives

Co-additives with phosphorous containing anchoring groups are generally believed to anchor strongly compared to carboxylic acid anchors. First example of such an additive was appeared in 2003 by Zakeerudin et al. when 1-decyl phosphonic acid (DPA, **Figure 9**) was used with a **Z-907** (a benchmark hydrophobic dye historically popular for stable devices) [111]. It was claimed as the first example of stable DSCs under heat stress and continuous illumination,

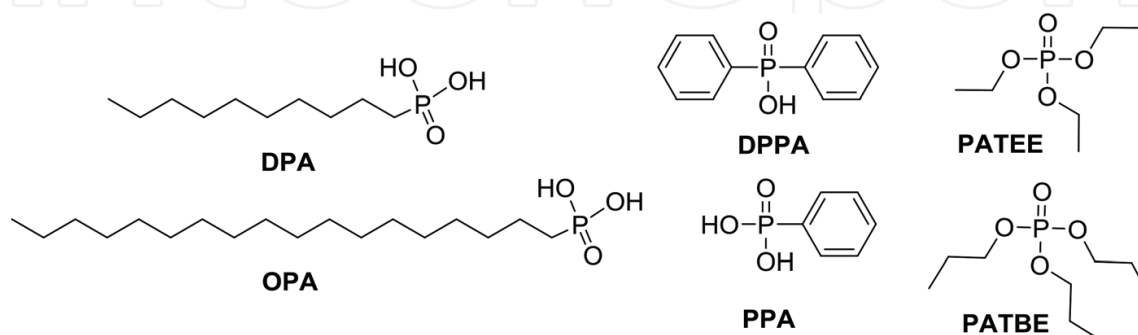


**Figure 9.** Representative additives.



with 7% increase in PCE due to DPA (4:1 dye/co-additive concentration was employed). Later on in a unique example octydecyl phosphonic acid (OPA) was also characterized for **Z-907** and cobalt redox shuttle [112].

OPA (18C) was found more effective in blocking recombination compared to DPA (10C) because of longer alkyl chain with overall 20% increase in PCE (8.4% versus 7% no OPA, **Figure 10**) with 18:1 (dye:OPA) concentration ratio. This is one of the highest efficiency reported so far for a Ru (II) dye containing NCS with cobalt redox shuttles, owing to inherently higher recombination losses [113–115].

In this class of co-additives, dineohexyl phosphinic acid (DINHOP, **Figure 11**) is known as an efficient molecular insulator to electronically passivate the oxide junctions such as TiO<sub>2</sub>, even outperforming CDCA in some comparative studies *vide infra* [105, 116]. DINHOP particularly benefits from the three dimensional orientation leading to better surface coverage [116]. Increase in PCE of 9% was realized for **Z-907** and DINHOP with 1:1 dye concentration (PCE 7.9% versus 7.24%).

In a comparative study for different small molecules (**Figure 9** containing phenylphosphonic acid (PPA), diphenylphosphinic acid (DPPA), phosphoric acid triethyl ester (PATEE), and phosphoric acid tributylester (PATBE) were employed as co-adsorbents [117]. It was found that alkyl chains performed better than the aromatic containing co-additives with ~12% enhancement in device PCE with **N719** sensitizer. The observed effect was established by EIS measurements (Nyquist plot), showing larger semicircle for high performing PATBE, pointing

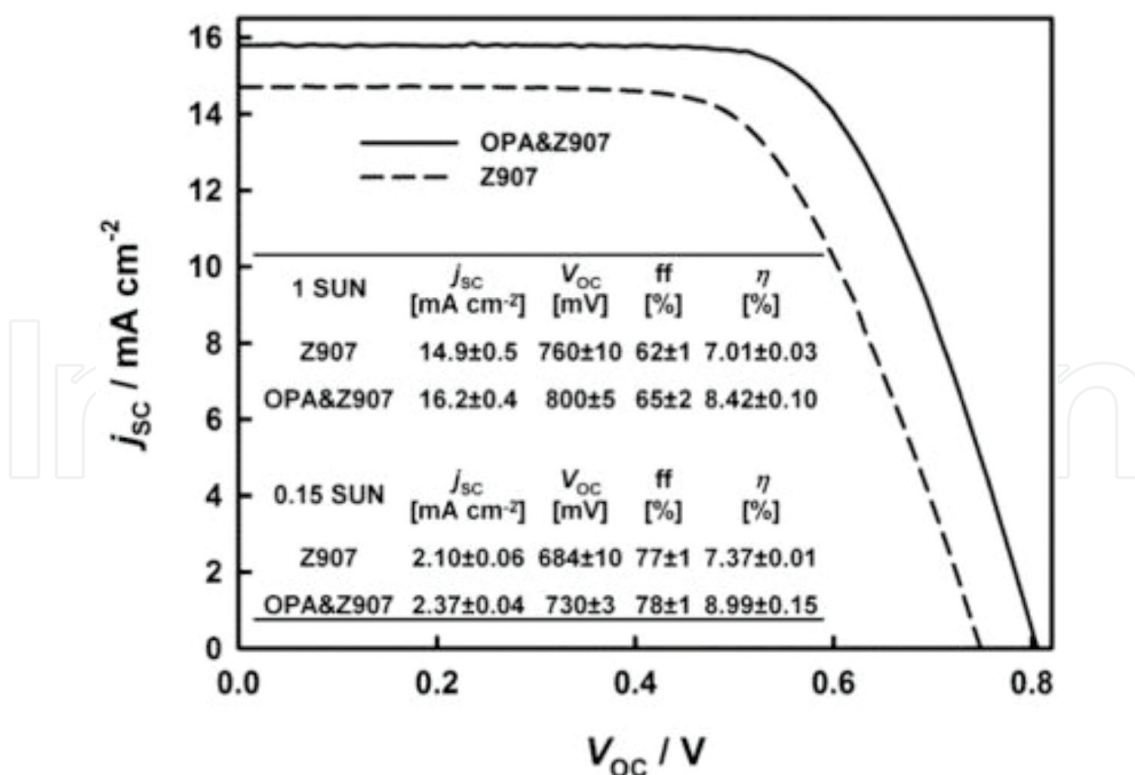


**Figure 10.** Effect of OPA on Z907 performance, taken from Ref. [66], with permission from The Royal Society of Chemistry.

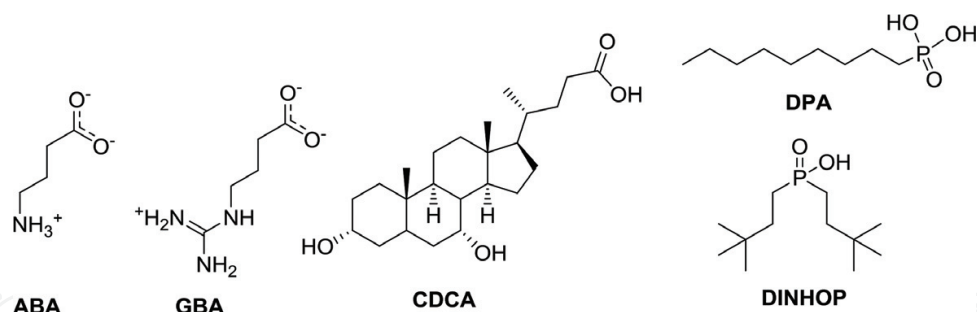


Figure 11. Co-additives employed in the comparative study.

to higher recombination resistance as the result of co-additive pretreatment of  $\text{TiO}_2$  film before dipping in dye solution.

4-guanidino butyric acid (GBA, **Figure 8**) was first time employed in 2005 by Grätzel group with a Ru (II) sensitizer **K19** [118]. In that detailed study, cyclic voltammetry was employed to determine the density of states (DOS), EIS to analyze interface charge transfer properties and photovoltage decay measurements for the effect of GAB on electron life time and capacitance of  $\text{TiO}_2$ . GBA was found to have similar kind of effect as t-butyl pyridine on  $\text{TiO}_2$  conduction band with negative shift in the quasi-fermi level of  $\text{TiO}_2$ . Additionally, increase in  $V_{oc}$  did not come as the result of decreased  $J_{sc}$ , thus leading to higher overall PCE (~9% increase with 1:1 concentration with the dye). In 2009, same group studied and compared GBA and 4-aminobutyric acid (ABA) for solid state DSCs and additives effect on long term stability (**Figure 11**) [101]. GBA outperformed ABA with about 37% increase in PCE compared to 16% decrease with ABA at 1:1 concentration. This was caused presumably due to more effective barrier formation to recombination and upward shift in the conduction band of  $\text{TiO}_2$  by GBA. Enhancement in device performance due to GBA was caused by 15% increase (113 mV) in  $V_{oc}$  and 18.5% increase in  $J_{sc}$ . GBA was also found to enhance the long term stability.

In a recent study based on **C106** dye, Chandiran et al. studied four different additives (**Figure 11**) for their potential effect on the  $\text{TiO}_2$  interface and device performance with different concentrations [105]. For **C106**, 4-guanidino butyric acid (GBA) resulted in 11% PCE, compared to 10.8% with CDCA at 0.5:1 (dye:CDCA) ratio compared to 6:1 for GBA (dye:GBA). In the same study, dineohexyl phosphinic acid (DINHOP) also showed slightly better results compared to CDCA (11% versus 10.8%), whereas dodecyl phosphonic acid (DPA) at 6:1 ratio marginally improved to 9.7% PCE. The device PCE without additives was reported to be 10.6%.

### 3.3. Dual function dyes as co-additives

An interesting approach to achieve multiple functionality such as light absorption and aggregation/recombination blocking at  $\text{TiO}_2$  surface is to employ small molecule organic light absorbing dyes along with main dye [119–122]. Few successful example of such yellow to orange dyes which can be termed as co-sensitizers and co-additives are shown in **Figure 12**. In a detailed study in 2011, it was shown that Y-shaped molecules such as **HC-A**, can

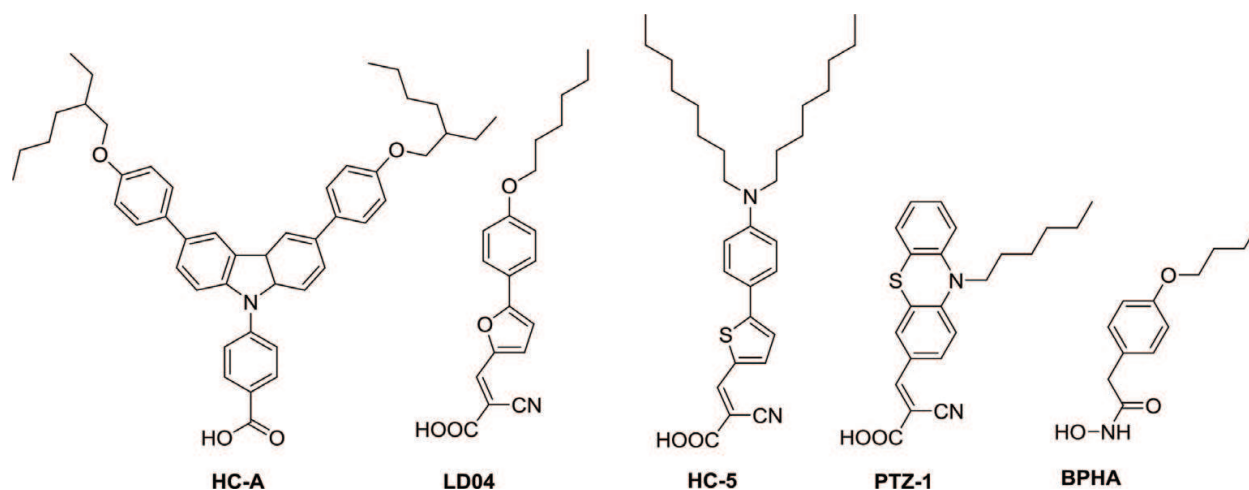


**Figure 12.** Small molecule co-sensitizing dyes as co-additives to modify TiO<sub>2</sub>.

potentially play multiple roles when co-adsorbed along with another organic dye (NKX2677) [119, 120]. IPCE confirmed the increased photocurrent response, EIS was used to rationalize the higher  $V_{oc}$  due to increased electron lifetime, and transient absorption studies showed the carbazole cation formation favorable for hole conduction. In a detailed study on similar lines with different molecules (HC3–5, **Figure 12**), black dye (BD) was optimized from 10.3% PCE to 11.3% for **BD + HC-5**, with 1:1 dye solution concentration [121]. As the result of co-sensitization, **BD + HC-5** mainly realized enhancement in  $J_{sc}$  (8.5%). It should be noted that CDA (chenodeoxycholic acid) as a co-adsorbent was also added in 100 times excess in this study. In a recent study, similar effects were claimed with **LD03** and **LD04** when co-sensitized along with **N719**. **N719 + LD04** showed highest enhancement of PCE from 7.896% to 8.955% (13.4% increase) due to better light harvesting, decrease in aggregation and higher electron recombination resistance [122]. **BPHA** (2-(4-butoxyphenyl)-N-hydroxyacetamide), **Figure 12**, was recently applied for chemical modification of TiO<sub>2</sub> before dye adsorption [123]. Though **BPHA**, was found to lower the adsorbed dye concentration, however, faster regeneration was reasoned for improved device performance (10–20%). Co-sensitizing approach of adsorbing multiple dyes on TiO<sub>2</sub> for enhanced light harvestings works on the same principles, in addition to order of staining, and dyes ratio, etc., interested readers are referred to the cited work [124–126].

#### 4. Post-staining surface treatment additives

To minimize the non-productive electron recombination pathways at the interface, chemical bath surface treatment of stained or dyed TiO<sub>2</sub> is a very effective approach (soft modification). Such that the highest reported efficiency DSCs (12–14.3%), applied the most extensive surface treatments known (**Figure 13**) [25, 53, 127, 128]. It should be noted that post staining surface treatment additive need to be inert towards the sensitizer, i.e., it should not impede light harvesting and detach it from the surface of TiO<sub>2</sub>. Surface treatment is less complex than co-additive approach and offer better control on treatment parameters such as concentration,

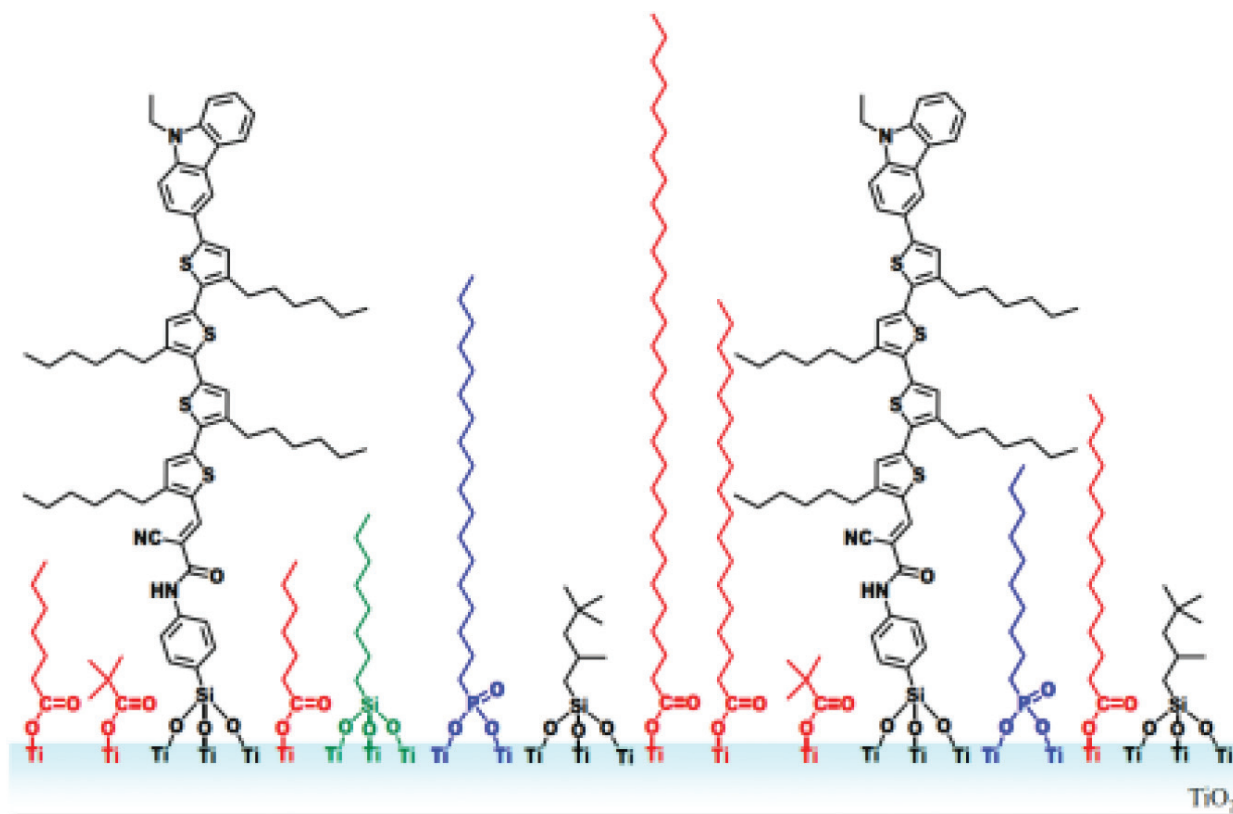


**Figure 13.** Post staining surface treatment example “alkyl-thicket” layer formation, adopted from Ref. [127], with permission from The Royal Society of Chemistry.

dipping time, etc. Below section highlights the most successful strategies categorized on the basis of anchoring groups.

#### 4.1. Carboxylic/phosphonic acid anchoring additives

Similar to dyes and co-adsorbing additives carboxylic/phosphonic acid anchoring groups are widely applied for surface treatment additives as well (**Figure 14**). Effect of long alkyl chain on enhancing electron lifetime in  $\text{TiO}_2$  was already known in conjunction with DSC sensitizers [129–131]. However, Hanaya et al. popularized the concept of “alkyl thicket” as an insulating barrier layer to block unwanted electron recombinations at  $\text{TiO}_2$ . As the result, overall device PCE increased impressively ~20% (9.44–11.3%), with increase in  $J_{sc}$  from 15.1 to 15.8  $\text{mA}/\text{cm}^2$  and increase in  $V_{oc}$  from 0.826 to 0.958 V (16% increase). It is interesting to note, the presence of long alkyl chains was not found to impede the charge transfer and diffusion with potentially favorable effect on long term stability as well [47]. These additives are usually applied in a hierarchical (stepwise) way with dipping in 0.1 M conc. (empirical) solution with the longest chain additives followed by small chain additives which can penetrate well in smaller cavities. In a very interesting study, a multifunctional methoxy-terminated oligomeric poly(ethylene glycol) (PEG) chain containing a carboxylic acid at one chain end (Mw - 2000) (*m*-PEG-succinic acid, **Figure 14**) is employed for post staining surface treatment [132]. The presence of electron rich oxygen atoms in *m*-PEG was claimed to favorably co-ordinate with vacant sites on  $\text{TiO}_2$



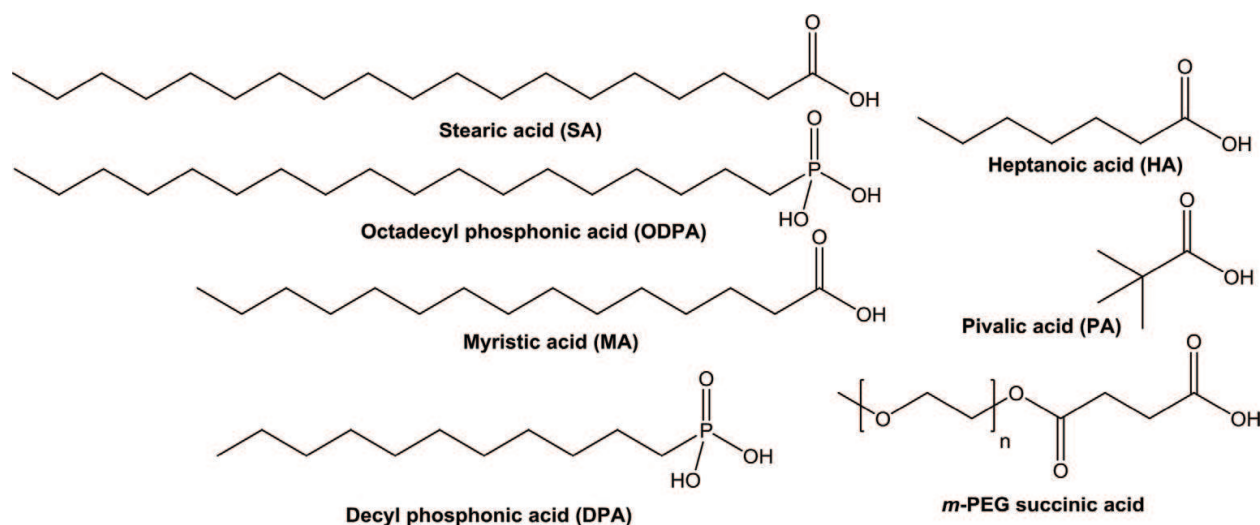


Figure 14. Additives used to modify  $\text{TiO}_2$  in post-staining fashion.

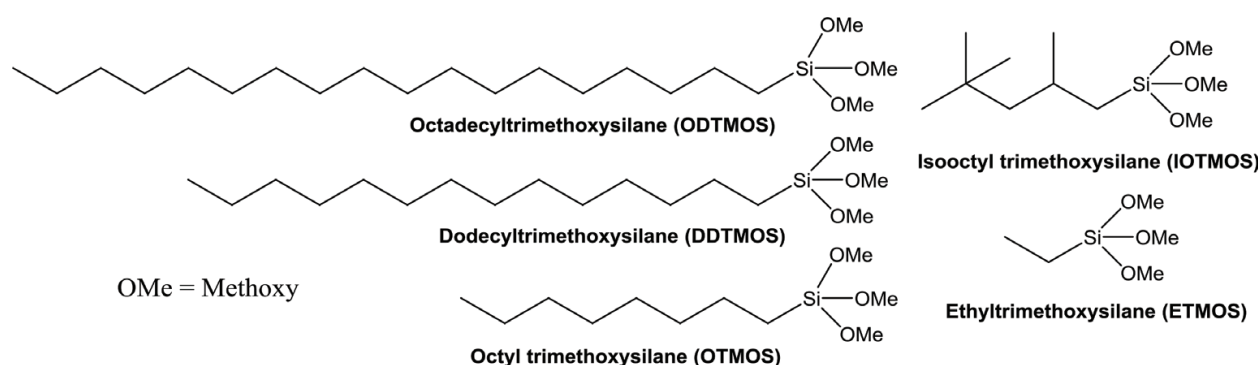


Figure 15. Alkoxy-silyl-based alkyl chain additives to modify  $\text{TiO}_2$ .

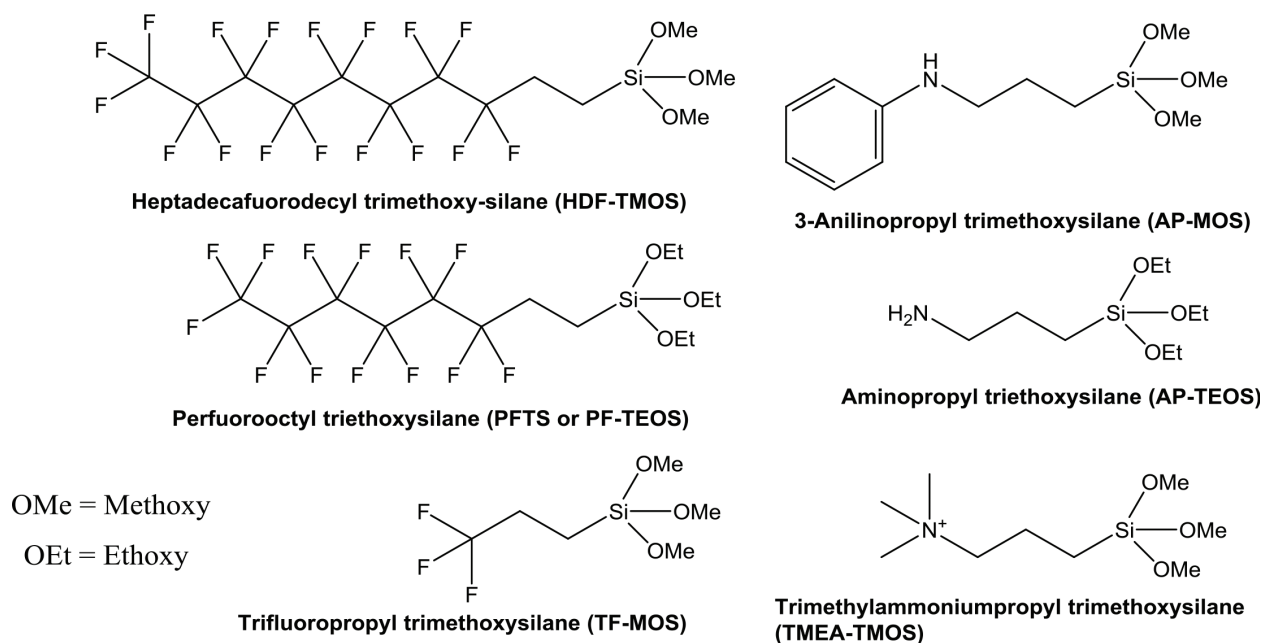
and worked collegially with common electrolyte additives such as  $\text{Li}^+$ , and tBP (4-terbutylpyridine). Increase in electron lifetime, decrease in dark current, and entrapment of  $\text{Li}^+$  resulted in both  $J_{sc}$  and  $V_{oc}$  enhancements.

## 4.2. Alkoxy-silyl-based anchoring additives

In addition to “alkyl thick” barrier layer for modifying  $\text{TiO}_2$  surface, Hanaya et al. also introduced and studied the silanol-based sensitizer and additives for  $\text{TiO}_2$  anchoring (Figures 13 and 15). It was found that titano-siloxane bonds are stronger and are more resistant to detachment from  $\text{TiO}_2$  compared to carboxylic acid anchors [127, 133]. However, it should be noted, other groups reported on the synthetic challenges related to the inclusion of siloxanes for DSC sensitizers [134].

An interesting and effective evolution is the replacement of hydrocarbon chain by fluorocarbon chain while keeping alkoxy-silyl anchoring groups the same (Figure 16) [135–138]. In the regime of organic PV's (OPVs) fluorinated alkyl chains has been effectively employed to result in surface segregated monolayer to achieve better charge transfer, polymer alignment and



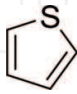
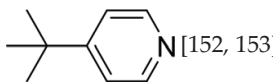
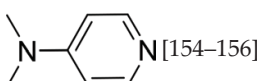
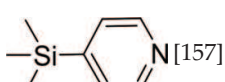
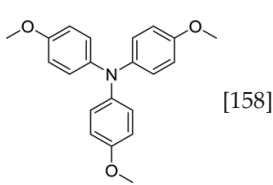
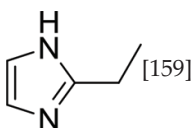
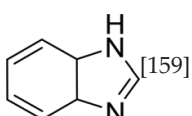


**Figure 16.** Alkoxysilyl and fluorocarbon based additives to modify TiO<sub>2</sub>.

direction of dipole moment at the interface [139–141]. For TiO<sub>2</sub> modification, detailed studies focused on unrevealing the impressive effect of fluorinated alkyl chains evidenced, enhanced electron lifetime in TiO<sub>2</sub>, de-aggregating behavior for organic dyes, negative (upward) conduction band shift of TiO<sub>2</sub> with metal complex dye, hydrophobicity and overall PCE enhancements presumably due to fluorinated self-assembled monolayer formation (FSAM) [53, 94, 142–145]. Interestingly, in one study, cationically charged TMEA-TMOS (**Figure 15**) outperformed C16 based alkyl chain analog when used with Ru (II) dye and cobalt redox shuttle. Detailed studies on unrevealing the structure–property relationship of such fluorocarbon chains for modifying TiO<sub>2</sub> are rare in literature at this stage.

## 5. Electrolyte additives

Electrolyte is an integral component of DSCs, and its composition has huge effect on performance, and long term stability. It consist of redox active species such as iodide/triiodide, Co (III)/Co(II), Fc (I)/Fc (0), and Cu (II)/Cu(I), etc., and certain additives which are known to adsorb on TiO<sub>2</sub> surface such as lithium cation (Li<sup>+</sup>), 4-ter butylpyridine (4-tBP) and guanidium thiocyanate (GuNCS) and others as shown in **Table 1** [160–162]. Source of Li<sup>+</sup> is mostly LiI for iodide/triiodide mediator and LiTfI or LiClO<sub>4</sub> for cobalt and copper based redox shuttles. Two widely studied redox systems for DSCs are iodide/triiodide and Co(III)/Co(II) with most recent as Cu(II)/Cu(I) [160–162]. Iodide/triiodide redox shuttle has been the favorable choice historically, but it results in lower photovoltage due to higher (less positive) redox potential, higher dye regeneration overpotential due to complex two step chemistry and corrosion of the DSCs components [160]. On the other hand, one electron redox shuttles such as cobalt and copper offer higher photovoltage, tunability, and less dye regeneration overpotential making them

No.	Additive	Conc. (M)	Electrolyte/dye	CB effect	Electron lifetime	$J_{sc}$	$V_{oc}$	PCE
1.	$\text{Li}^+$ [146]	0.05–0.5	I/Co	Down	Inc.	Inc.	Dec.	Inc.
2	CDCA [147]	0.1	Co/Ru (II)	Inc.	Inc.	Inc.	Inc.	Inc.
3	$\text{Li}_2\text{CO}_3$ [148]	0.0025	I/Ru (II)	Up	Inc.	Inc.	Inc.	Inc.
4	$\text{K}_2\text{CO}_3$ [148]	0.05	I/Ru (II)	Up	Inc.	Inc.	Inc.	Inc.
5	GuNCS [149]	0.1	I	Down	Dec.	Inc.	Dec.	Inc.
6	GuNO <sub>3</sub> [150]	0.1	I	Up	Inc.	Inc.	Inc.	Inc.
7	 [151]	1	I/Ru (II)	Down	Dec.	Inc.	Dec.	Inc.
8	 [152, 153]	0.25–0.5	I/Co	Up	Inc.	Dec.	Inc.	Inc.
9	 [154–156]	0.5	I/Ru (II)	Up	Inc.	Dec.	Inc.	Dec.
10	 [157]	0.5	Co	Up	Inc.	Dec.	Inc.	Inc.
11	 [158]	0.1	Co	Up	Inc.	Inc.	Inc.	Inc.
12	 [159]	0.5	I/Ru (II)	Up	Inc.	Dec.	Inc.	Inc.
13	 [159]	0.5	I/Ru (II)	Up	Inc.	Dec.	Inc.	Dec.

Up = upward shift, Down = downward shift, Inc. = increase, and Dec. = decrease.

**Table 1.** Summarizing the effect of electrolyte additives effect on TiO<sub>2</sub> and DSC parameters.

popular for recent studies [52, 163]. For iodide/triiodide most commonly employed additives are  $\text{Li}^+$ , GuNCS and 4-tBP, whereas one electron redox shuttles mainly employ  $\text{Li}^+$  and 4-tBP only. Generally speaking, cationic additives charge the TiO<sub>2</sub> surface positively thus lowering the conduction band (**Table 1**, entry 1) [56, 146]. Electron rich or nitrogen containing additives on the other hand charge the TiO<sub>2</sub> surface negatively or increase electron density thus raising the conduction band, blocking the recombination and resulting in higher  $V_{oc}$ . An important factor is the concentration which is commonly optimized empirically such as for  $\text{Li}_2\text{CO}_3$ , GuNO<sub>3</sub>, etc., additives [148, 150]. Electrolyte additives and their known effect in terms of TiO<sub>2</sub> modification and subsequent DSC device parameters are shown in **Table 1**.

Since NCS containing Ru (II) sensitizers are incompatible with cobalt, inclusion of CDCA (**Table 1**, entry 2) substantially lowered the recombination losses and increased the PCE from 1.9 to 5.7% [147]. An interesting study, was the inclusion of  $\text{Li}_2\text{CO}_3$  and  $\text{K}_2\text{CO}_3$  (**Table 1**, entries 3 and 4) as a source of  $\text{Li}^+$ , where former outperformed latter [148].  $\text{Li}_2\text{CO}_3$  enhanced the device performance (6.5–7.6%) without lowering  $V_{oc}$ , presumably due to formation of carbonate layer on  $\text{TiO}_2$ , as evidenced by FT-IR. In a comparative study,  $\text{GuNO}_3$  showed overall better performance compared to well-known  $\text{GuNCS}$ , without negative effect on  $V_{oc}$  [150]. It was supported by the favorable effect of  $\text{NO}_3^-$  on  $\text{TiO}_2$  CB (upward shift), which was not observed for  $\text{NCS}^-$  without affecting diffusion negatively. Thiophene (**Table 1**, entry 7) when added in 1 M concentration had  $\text{Li}^+$  like effect to enhance the  $J_{sc}$  [151]. 4-tBP (**Table 1**, entries 8–10) and its derivatives such as methyl pyridine, pyrimidine, pyrazole, triazole, thiazole and quinolone has been extensively explored by Arakawa et al. [154, 164–167]. Out of these, 4-trimethylsilylpyridine (**Table 1**, entry 10), have particularly shown better overall performance due to its bulkiness to block recombination reaction at interface, and better electron donating ability without negatively effecting the electron injection [157]. In a recent study, tris(4-methoxyphenyl)amine (TPAA, **Table 1** entry 11) as an electron donor was explored by Boschloo et al. [158].

The inclusion of TPAA in cobalt electrolyte particularly blocked the recombination with oxidized sensitizer which lead to 26% increase in the DSC performance. 2-ethylimidazole and benzimidazole (**Table 1**, entries 12 and 13) due to labile proton and lone pairs on electron were expected to be good coordinating candidates to modify  $\text{TiO}_2$  as studied by Wei et al. [159]. Benzimidazole and 2-ethylimidazole were found to perform best when employed in the molar ratio of 9.5/0.5 respectively (7.93% PCE compared to 6.8%). These additives showed pyridine type effect in modifying  $\text{TiO}_2$ . To this point, only few reports are available on the long term stability effect of these additives on  $\text{TiO}_2$  properties and DSC device performance [168, 169].

In this chapter, DSC electrolyte additives are discussed with respect to liquid based systems, whereas liquid in these electrolytes eventually has to be replaced for long term stability either by solid or semi-solid (gel type) systems. Reader are kindly referred to the published literature for semisolid gel type electrolyte which generally apply similar additives and offer better long term stability [162, 170–172].

## 6. Summary

In summary, this chapter aimed at recognizing and highlighting various approaches to modify  $\text{TiO}_2$  material based on the studies focusing on dye-sensitized solar cells. The emphasis was to identify the most successful examples and to rationalize their effect in enhancing electronic mobility, charge carrier generation and diffusion, conduction band shift, surface passivation, light harvesting, long term stability and ease of application. In general,  $\text{TiO}_2$  modification can be categorized into hard modification and soft modification. Hard modification involves the addition of moieties such as plasmonic nanostructures, metal oxides, and morphological variations during synthesis such as a high temperature sintering (400–500°C) step is required

to achieve required functionality. On the other hand, soft modification (simple rinse and dry) post sintering surface treatment with additives, co-adsorbents, and electrolyte additives is rather simple to apply. With the discussion and literature provided in the chapter we hope the state of knowledge learned from dye-sensitized solar cells will benefit the scientific community to expand on the functionality of  $\text{TiO}_2$  as it is being applied and explored in the fields of energy storage (batteries, super capacitors), photocatalysis, PVs, and sensors.

## Author details

Hammad Cheema<sup>1\*</sup> and Khurram S. Joya<sup>2,3</sup>

\*Address all correspondence to: hac@go.olemiss.edu

1 Chemistry Department, University of Mississippi, MS, USA

2 Department of Energy Conversion and Storage, Technical University of Denmark, Roskilde, Denmark

3 Department of Chemistry, University of Engineering and Technology (UET), Lahore, Punjab, Pakistan

## References

- [1] Joya KS, Joya YF, Ocakoglu K, van de Krol R. Water-splitting catalysis and solar fuel devices: Artificial leaves on the move. *Angewandte Chemie, International Edition*. 2013; **52**(40):10426-10437
- [2] Outlook WE. World energy outlook 2015. International Energy Agency. 2015
- [3] Colton W. The Outlook for Energy: A View to 2040. Exxon Mobil Corporation; 2011
- [4] Olah GA. Beyond oil and gas: The methanol economy. *Angewandte Chemie, International Edition*. 2005; **44**(18):2636-2639
- [5] Chu S, Majumdar A. Opportunities and challenges for a sustainable energy future. *Nature*. 2012; **488**(7411):294-303
- [6] Turner JA. Sustainable hydrogen production. *Science*. 2004; **305**(5686):972-974
- [7] Joya KS, Morlanes N, Maloney E, Rodionov V, Takanabe K. Immobilization of a molecular cobalt electrocatalyst by hydrophobic interaction with a hematite photoanode for highly stable oxygen evolution. *Chemical Communications*. 2015; **51**(70):13481-13484
- [8] Ocakoglu K, Joya KS, Harputlu E, Tarnowska A, Gryko DT. A nanoscale bio-inspired light-harvesting system developed from self-assembled alkyl-functionalized metallochlorin nano-aggregates. *Nanoscale*. 2014; **6**(16):9625-9631

- [9] Lewis NS, Nocera DG. Powering the planet: Chemical challenges in solar energy utilization. *Proceedings of the National Academy of Sciences*. 2006;**103**(43):15729-15735
- [10] Feltrin A, Freundlich A. Material considerations for terawatt level deployment of photovoltaics. *Renewable Energy*. 2008;**33**(2):180-185
- [11] O'Regan B, Grätzel M. A low-cost, high-efficiency solar cell based on dye-sensitized colloidal TiO<sub>2</sub> films. *Nature*. 1991;**353**(6346):737-740
- [12] Hagfeldt A, Boschloo G, Sun L, Kloo L, Pettersson H. Dye-sensitized solar cells. *Chemical Reviews*. 2010;**110**(11):6595-6663
- [13] Gratzel M. Photoelectrochemical cells. *Nature*. 2001;**414**(6861):338-344
- [14] Grätzel M. Recent advances in sensitized mesoscopic solar cells. *Accounts of Chemical Research*. 2009;**42**(11):1788-1798
- [15] Kalyanasundaram K. *Dye-sensitized Solar Cells*. Boca Raton, Fla.; London: CRC; Taylor & Francis [distributor]; 2009
- [16] Kavan L, Grätzel M, Gilbert SE, Klemenz C, Scheel HJ. Electrochemical and photoelectrochemical investigation of single-crystal anatase. *Journal of the American Chemical Society*. 1996;**118**(28):6716-6723
- [17] Carp O, Huisman CL, Reller A. Photoinduced reactivity of titanium dioxide. *Progress in Solid State Chemistry*. 2004;**32**(1):33-177
- [18] Dambournet D, Belharouak I, Amine K. Tailored preparation methods of TiO<sub>2</sub> anatase, rutile, brookite: Mechanism of formation and electrochemical properties. *Chemistry of Materials*. 2010;**22**(3):1173-1179
- [19] Yang WS, Noh JH, Jeon NJ, Kim YC, Ryu S, Seo J, et al. High-performance photovoltaic perovskite layers fabricated through intramolecular exchange. *Science*. 2015
- [20] Gratzel M. The light and shade of perovskite solar cells. *Nature Materials*. 2014;**13**(9):838-842
- [21] Mishra A, Fischer MKR, Bäuerle P. Metal-free organic dyes for dye-sensitized solar cells: from structure: Property relationships to design rules. *Angewandte Chemie, International Edition*. 2009;**48**(14):2474-2499
- [22] Zhang S, Yang X, Numata Y, Han L. Highly efficient dye-sensitized solar cells: Progress and future challenges. *Energy & Environmental Science*. 2013;**6**(5):1443-1464
- [23] Ahmad S, Guillen E, Kavan L, Gratzel M, Nazeeruddin MK. Metal free sensitizer and catalyst for dye sensitized solar cells. *Energy & Environmental Science*. 2013;**6**(12):3439-3466
- [24] Ardo S, Meyer GJ. Photodriven heterogeneous charge transfer with transition-metal compounds anchored to TiO<sub>2</sub> semiconductor surfaces. *Chemical Society Reviews*. 2009;**38**(1):115-164



- [25] Kakiage K, Aoyama Y, Yano T, Oya K, Fujisawa J-i, Hanaya M. Highly-efficient dye-sensitized solar cells with collaborative sensitization by silyl-anchor and carboxy-anchor dyes. *Chemical Communications*. 2015;**51**(88):15894-15897
- [26] Li J-Y, Chen C-Y, Ho W-C, Chen S-H, Wu C-G. Unsymmetrical squaraines incorporating quinoline for near infrared responsive dye-sensitized solar cells. *Organic Letters*. 2012;**14**(21):5420-5423
- [27] Liyanage NP, Yella A, Nazeeruddin M, Grätzel M, Delcamp JH. Thieno[3,4-b]pyrazine as an electron deficient  $\pi$ -bridge in D-A- $\pi$ -A DSCs. *ACS Applied Materials & Interfaces*. 2016;**8**(8):5376-5384
- [28] Lu X, Zhou G, Wang H, Feng Q, Wang ZS. Near infrared thieno[3,4-b]pyrazine sensitizers for efficient quasi-solid-state dye-sensitized solar cells. *Physical Chemistry Chemical Physics (PCCP)*. 2012;**14**(14):4802-4809
- [29] Wu J, Li G, Zhang L, Zhou G, Wang Z-S. Energy level engineering of thieno[3,4-b]pyrazine based organic sensitizers for quasi-solid-state dye-sensitized solar cells. *Journal of Materials Chemistry A*. 2016;**4**(9):3342-3355
- [30] Ito S, Murakami TN, Comte P, Liska P, Grätzel C, Nazeeruddin MK, et al. Fabrication of thin film dye sensitized solar cells with solar to electric power conversion efficiency over 10%. 6th International Conference on Coatings on Glass and Plastics (ICCG6). *Advanced Coatings for Large-Area or High-Volume Products*. 2008;**516**(14):4613-4619
- [31] Yella A, Mathew S, Aghazada S, Comte P, Gratzel M, Nazeeruddin MK. Dye-sensitized solar cells using cobalt electrolytes: The influence of porosity and pore size to achieve high-efficiency. *Journal of Materials Chemistry C*. 2017;**5**(11):2833-2843
- [32] Cheema H, Ogbose L, El-Shafei A. Structure–property relationships: Steric effect in ancillary ligand and how it influences photocurrent and photovoltage in dye-sensitized solar cells. *Dyes and Pigments*. 2015;**113**(0):151-159
- [33] Yum J-H, Baranoff E, Wenger S, Nazeeruddin MK, Grätzel M. Panchromatic engineering for dye-sensitized solar cells. *Energy & Environmental Science*. 2011;**4**(3):842-857
- [34] Pazoki M, Cappel UB, Johansson EMJ, Hagfeldt A, Boschloo G. Characterization techniques for dye-sensitized solar cells. *Energy & Environmental Science*. 2017;**10**(3):672-709
- [35] Ning Z, Fu Y, Tian H. Improvement of dye-sensitized solar cells: What we know and what we need to know. *Energy & Environmental Science*. 2010;**3**(9):1170-1181
- [36] Hardin BE, Snaith HJ, McGehee MD. The renaissance of dye-sensitized solar cells. *Nature Photonics*. 2012;**6**(3):162-169
- [37] Cheema H, Islam A, Han L, El-Shafei A. Monodentate pyrazole as a replacement of labile NCS for Ru (II) photosensitizers: Minimum electron injection free energy for dye-sensitized solar cells. *Dyes and Pigments*. 2015;**120**:93-98

- [38] Cheema H, Islam A, Han L, Gautam B, Younts R, Gundogdu K, et al. Influence of mono versus bis-electron-donor ancillary ligands in heteroleptic Ru(ii) bipyridyl complexes on electron injection from the first excited singlet and triplet states in dye-sensitized solar cells. *Journal of Materials Chemistry A*. 2014;**2**(34):14228-14235
- [39] Liyanage NP, Cheema H, Baumann AR, Zylstra AR, Delcamp JH. Effect of donor strength and bulk on thieno[3,4-b]-pyrazine-based panchromatic dyes in dye-sensitized solar cells. *ChemSusChem*. 2017;**10**:2635-2641
- [40] Brogdon P, Cheema H, Delcamp JH. Low-recombination thieno[3,4-b]thiophene-based photosensitizers for dye-sensitized solar cells with panchromatic photoresponses. *ChemSusChem*. 2017;**10**(18):3624-3631
- [41] Brogdon P, Cheema H, Delcamp JH. NIR absorbing metal-free organic, porphyrin, and phthalocyanine dyes for panchromatic DSCs. *ChemSusChem*. n/a-n/a
- [42] Wu Y, Zhu W. Organic sensitizers from D- $\pi$ -A to D-A- $\pi$ -A: Effect of the internal electron-withdrawing units on molecular absorption, energy levels and photovoltaic performances. *Chemical Society Reviews*. 2013;**42**(5):2039-2058
- [43] Wu Y, Zhu WH, Zakeeruddin SM, Gratzel M. Insight into D-A- $\pi$ -A structured sensitizers: A promising route to highly efficient and stable dye-sensitized solar cells. *ACS Applied Materials & Interfaces*. 2015;**7**(18):9307
- [44] Ito S, Dharmadasa IM, Tolan GJ, Roberts JS, Hill G, Miura H, et al. High-voltage (1.8 V) tandem solar cell system using a GaAs/Al<sub>x</sub>Ga(1-x)As graded solar cell and dye-sensitized solar cells with organic dyes having different absorption spectra. *Solar Energy*. 2011;**85**(6):1220-1225
- [45] Fabregat-Santiago F, Bisquert J, Garcia-Belmonte G, Boschloo G, Hagfeldt A. Influence of electrolyte in transport and recombination in dye-sensitized solar cells studied by impedance spectroscopy. *International Conference on Physics, Chemistry and Engineering*. 2005;**87**(1-4):117-131
- [46] Koide N, Islam A, Chiba Y, Han L. Improvement of efficiency of dye-sensitized solar cells based on analysis of equivalent circuit. *Journal of Photochemistry and Photobiology A: Chemistry; Proceedings of 7th AIST International Symposium on Photoreaction Control and Photofunctional Materials 7th AIST International Symposium on Photoreaction Control and Photofunctional Materials*. 2006;**182**(3):296-305
- [47] Cheema H, Islam A, Younts R, Gautam B, Bedja I, Gupta RK, et al. More stable and more efficient alternatives of Z-907: Carbazole-based amphiphilic Ru(ii) sensitizers for dye-sensitized solar cells. *Physical Chemistry Chemical Physics*. 2014;**16**(48):27078-27087
- [48] Barnes PRF, Miettunen K, Li X, Anderson AY, Bessho T, Grätzel M, et al. Interpretation of optoelectronic transient and charge extraction measurements in dye-sensitized solar cells. *Advanced Materials*. 2013;**25**(13):1881-1922

- [49] Zhang L, Cole JM. Anchoring groups for dye-sensitized solar cells. *ACS Applied Materials & Interfaces*. 2015;7:3427-3455
- [50] Deacon GB, Phillips RJ. Relationships between the carbon-oxygen stretching frequencies of carboxylato complexes and the type of carboxylate coordination. *Coordination Chemistry Reviews*. 1980;33(3):227-250
- [51] Kalyanasundaram K, Grätzel M. Applications of functionalized transition metal complexes in photonic and optoelectronic devices. *Coordination Chemistry Reviews*. 1998;177(1):347-414
- [52] Freitag M, Teuscher J, Saygili Y, Zhang X, Giordano F, Liska P, et al. Dye-sensitized solar cells for efficient power generation under ambient lighting. *Nature Photonics*. 2017;11(6):372-378
- [53] Cheema H, Rodrigues RR, Delcamp JH. Sequential series multijunction dye-sensitized solar cells (SSM-DSCs): 4.7 volts from a single illuminated area. *Energy & Environmental Science*. 2017;10(8):1764-1769
- [54] Feldt SM, Gibson EA, Gabrielsson E, Sun L, Boschloo G, Hagfeldt A. Design of organic dyes and cobalt polypyridine redox mediators for high-efficiency dye-sensitized solar cells. *Journal of the American Chemical Society*. 2010;132(46):16714-16724
- [55] Fakharuddin A, Jose R, Brown TM, Fabregat-Santiago F, Bisquert J. A perspective on the production of dye-sensitized solar modules. *Energy & Environmental Science*. 2014;7(12):3952-3981
- [56] Bai Y, Mora-Seró I, De Angelis F, Bisquert J, Wang P. Titanium dioxide nanomaterials for photovoltaic applications. *Chemical Reviews*. 2014;114(19):10095-10130
- [57] Li Z-Q, Chen W-C, Guo F-L, Mo L-E, Hu L-H, Dai S-Y. Mesoporous TiO<sub>2</sub> yolk-shell microspheres for dye-sensitized solar cells with a high efficiency exceeding 11%. *Scientific Reports*. 2015;5:14178
- [58] Li Z-Q, Ding Y, Mo L-E, Hu L-H, Wu J-H, Dai S-Y. Fine tuning of nanocrystal and pore sizes of TiO<sub>2</sub> submicrospheres toward high performance dye-sensitized solar cells. *ACS Applied Materials & Interfaces*. 2015;7(40):22277-22283
- [59] Wen C, Ishikawa K, Kishima M, Yamada K. Effects of silver particles on the photovoltaic properties of dye-sensitized TiO<sub>2</sub> thin films. *Solar Energy Materials and Solar Cells*. 2000;61(4):339-351
- [60] Choi H, Chen WT, Kamat PV. Know thy nano neighbor. Plasmonic versus electron charging effects of metal nanoparticles in dye-sensitized solar cells. *ACS Nano*. 2012;6(5):4418-4427
- [61] Dang X, Qi J, Klug MT, Chen P-Y, Yun DS, Fang NX, et al. Tunable localized surface plasmon-enabled broadband light-harvesting enhancement for high-efficiency panchromatic dye-sensitized solar cells. *Nano Letters*. 2013;13(2):637-642

- [62] Erwin WR, Zarick HF, Talbert EM, Bardhan R. Light trapping in mesoporous solar cells with plasmonic nanostructures. *Energy & Environmental Science*. 2016;**9**(5):1577-1601
- [63] Maier SA. *Plasmonics: Fundamentals and Applications*. Springer Science & Business Media; 2007
- [64] Novotny L, Van Hulst N. Antennas for light. *Nature Photonics*. 2011;**5**(2):83-90
- [65] Xu Q, Liu F, Meng W, Huang Y. Plasmonic core-shell metal-organic nanoparticles enhanced dye-sensitized solar cells. *Optics Express*. 2012;**20**(S6):A898-A907
- [66] Li Y, Wang H, Feng Q, Zhou G, Wang Z-S. Gold nanoparticles inlaid TiO<sub>2</sub> photoanodes: A superior candidate for high-efficiency dye-sensitized solar cells. *Energy & Environmental Science*. 2013;**6**(7):2156-2165
- [67] Adhyaksa GWP, Baek S-W, Lee GI, Lee DK, Lee J-Y, Kang JK. Coupled near- and far-field scattering in silver nanoparticles for high-efficiency, stable, and thin plasmonic dye-sensitized solar cells. *ChemSusChem*. 2014;**7**(9):2461-2468
- [68] Zheng D, Pang X, Wang M, He Y, Lin C, Lin Z. Unconventional route to hairy plasmonic/semiconductor core/shell nanoparticles with precisely controlled dimensions and their use in solar energy conversion. *Chemistry of Materials*. 2015;**27**(15):5271-5278
- [69] Liu M, Yin X, Ulin-Avila E, Geng B, Zentgraf T, Ju L, et al. A graphene-based broadband optical modulator. *Nature*. 2011;**474**(7349):64
- [70] Akimov YA, Koh W. Resonant and nonresonant plasmonic nanoparticle enhancement for thin-film silicon solar cells. *Nanotechnology*. 2010;**21**(23):235201
- [71] Chen X, Jia B, Zhang Y, Gu M. Exceeding the limit of plasmonic light trapping in textured screen-printed solar cells using Al nanoparticles and wrinkle-like graphene sheets. *Light: Science and Applications*. 2013;**2**(8):e92
- [72] Hwang E, Sarma SD. Dielectric function, screening, and plasmons in two-dimensional graphene. *Physical Review B*. 2007;**75**(20):205418
- [73] Comin A, Manna L. New materials for tunable plasmonic colloidal nanocrystals. *Chemical Society Reviews*. 2014;**43**(11):3957-3975
- [74] Liu X, Swihart MT. Heavily-doped colloidal semiconductor and metal oxide nanocrystals: An emerging new class of plasmonic nanomaterials. *Chemical Society Reviews*. 2014;**43**(11):3908-3920
- [75] Jose R, Thavasi V, Ramakrishna S. Metal oxides for dye-sensitized solar cells. *Journal of the American Ceramic Society*. 2009;**92**(2):289-301
- [76] Shakeel Ahmad M, Pandey AK, Abd Rahim N. Advancements in the development of TiO<sub>2</sub> photoanodes and its fabrication methods for dye sensitized solar cell (DSSC) applications. A review. *Renewable and Sustainable Energy Reviews*. 2017;**77**(Supplement C):89-108



- [77] Feng X, Zhu K, Frank AJ, Grimes CA, Mallouk TE. Rapid charge transport in dye-sensitized solar cells made from vertically aligned single-crystal rutile TiO<sub>2</sub> nanowires. *Angewandte Chemie*. 2012;**124**(11):2781-2784
- [78] Feng X, Shankar K, Varghese OK, Paulose M, Latempa TJ, Grimes CA. Vertically aligned single crystal TiO<sub>2</sub> nanowire arrays grown directly on transparent conducting oxide coated glass: Synthesis details and applications. *Nano Letters*. 2008;**8**(11):3781-3786
- [79] Fattakhova-Rohlfing D, Zaleska A, Bein T. Three-dimensional titanium dioxide nanomaterials. *Chemical Reviews*. 2014;**114**(19):9487-9558
- [80] Mor GK, Varghese OK, Paulose M, Shankar K, Grimes CA. A review on highly ordered, vertically oriented TiO<sub>2</sub> nanotube arrays: Fabrication, material properties, and solar energy applications. *Solar Energy Materials and Solar Cells*. 2006;**90**(14):2011-2075
- [81] Zhou Q, Fang Z, Li J, Wang M. Applications of TiO<sub>2</sub> nanotube arrays in environmental and energy fields: A review. *Microporous and Mesoporous Materials*. 2015;**202**(Supplement C):22-35
- [82] Lin J, Peng Y, Pascoe AR, Huang F, Cheng Y-B, Heo Y-U, et al. A bi-layer TiO<sub>2</sub> photoanode for highly durable, flexible dye-sensitized solar cells. *Journal of Materials Chemistry A*. 2015;**3**(8):4679-4686
- [83] Lee CS, Kim JK, Lim JY, Kim JH. One-step process for the synthesis and deposition of anatase, two-dimensional, disk-shaped TiO<sub>2</sub> for dye-sensitized solar cells. *ACS Applied Materials & Interfaces*. 2014;**6**(23):20842-20850
- [84] Deepak TG, Anjusree GS, Pai KRN, Subash D, Nair SV, Nair AS. Cabbage leaf-shaped two-dimensional TiO<sub>2</sub> mesostructures for efficient dye-sensitized solar cells. *RSC Advances*. 2014;**4**(51):27084-27090
- [85] Oh J-K, Lee J-K, Kim H-S, Han S-B, Park K-W. TiO<sub>2</sub> branched nanostructure electrodes synthesized by seeding method for dye-sensitized solar cells. *Chemistry of Materials*. 2010;**22**(3):1114-1118
- [86] Roh DK, Chi WS, Jeon H, Kim SJ, Kim JH. High efficiency solid-state dye-sensitized solar cells assembled with hierarchical anatase pine tree-like TiO<sub>2</sub> nanotubes. *Advanced Functional Materials*. 2014;**24**(3):379-386
- [87] Kim H-B, Kim H, Lee WI, Jang D-J. Hierarchical mesoporous anatase TiO<sub>2</sub> nanostructures with efficient photocatalytic and photovoltaic performances. *Journal of Materials Chemistry A*. 2015;**3**(18):9714-9721
- [88] Roose B, Pathak S, Steiner U. Doping of TiO<sub>2</sub> for sensitized solar cells. *Chemical Society Reviews*. 2015;**44**(22):8326-8349
- [89] Lee J-J, Rahman MM, Sarker S, Nath ND, Ahammad AS, Lee JK. Metal oxides and their composites for the photoelectrode of dye sensitized solar cells. In: *Advances in Composite Materials for Medicine and Nanotechnology*. Rijeka: InTech; 2011



- [90] Peng T, Fan K, Zhao D, Chen J. Enhanced energy conversion efficiency of  $\text{Mg}^{2+}$ -modified mesoporous  $\text{TiO}_2$  nanoparticles electrodes for dye-sensitized solar cells. *The Journal of Physical Chemistry C*. 2010;**114**(50):22346-22351
- [91] Kakiage K, Osada H, Aoyama Y, Yano T, Oya K, Iwamoto S, et al. Achievement of over 1.4 V photovoltage in a dye-sensitized solar cell by the application of a silyl-anchor coumarin dye. *Scientific Reports*. 2016;**6**:35888
- [92] Kakiage K, Tokutome T, Iwamoto S, Kyomen T, Hanaya M. Fabrication of a dye-sensitized solar cell containing a Mg-doped  $\text{TiO}_2$  electrode and a  $\text{Br}^{3-}/\text{Br}^-$  redox mediator with a high open-circuit photovoltage of 1.21 V. *Chemical Communications*. 2013;**49**(2):179-180
- [93] Zhang C, Chen S, Mo L, Huang Y, Tian H, Hu L, et al. Charge recombination and band-edge shift in the dye-sensitized  $\text{Mg}^{2+}$ -doped  $\text{TiO}_2$  solar cells. *The Journal of Physical Chemistry C*. 2011;**115**(33):16418-16424
- [94] Cheema H, Delcamp JH. Harnessing photovoltage: Effects of film thickness,  $\text{TiO}_2$  nanoparticle size, MgO and surface capping with DSCs. *ACS Applied Materials & Interfaces*. 2017;**9**(3):3050-3059
- [95] Miyasaka T, Watanabe T, Fujishima A, Honda K. Light energy conversion with chlorophyll monolayer electrodes. In vitro electrochemical simulation of photosynthetic primary processes. *Journal of the American Chemical Society*. 1978;**100**(21):6657-6665
- [96] Kay A, Graetzel M. Artificial photosynthesis. 1. Photosensitization of titania solar cells with chlorophyll derivatives and related natural porphyrins. *The Journal of Physical Chemistry*. 1993;**97**(23):6272-6277
- [97] Ogunsolu OO, Murphy IA, Wang JC, Das A, Hanson K. Energy and electron transfer cascade in self-assembled bilayer dye-sensitized solar cells. *ACS Applied Materials & Interfaces*. 2016;**8**(42):28633-28640
- [98] Manthou VS, Pefkianakis EK, Falaras P, Vougioukalakis GC. Co-adsorbents: A key component in efficient and robust dye-sensitized solar cells. *ChemSusChem*. 2015;**8**(4):588-599
- [99] Delcamp JH, Shi Y, Yum JH, Sajoto T, Dell'Orto E, Barlow S, et al. The role of  $\pi$ -bridges in high-efficiency DSCs based on unsymmetrical squaraines. *Chemistry - A European Journal*. 2013;**19**:1819-1827
- [100] Reynal A, Palomares E. Increasing the performance of cis-dithiocyanato (4, 4'-dicarboxy-2, 2'-bipyridine)(1, 10-phenanthroline) ruthenium (ii) based DSC using citric acid as co-adsorbant. *Energy & Environmental Science*. 2009;**2**(10):1078-1081
- [101] Wang M, Grätzel C, Moon S-J, Humphry-Baker R, Rossier-Iten N, Zakeeruddin SM, et al. Surface design in solid-state dye sensitized solar cells: effects of zwitterionic co-adsorbents on photovoltaic performance. *Advanced Functional Materials*. 2009;**19**(13):2163-2172

- [102] Peddapuram A, Cheema H, Adams RE, Schmehl RH, Delcamp JH. A stable panchromatic green dual acceptor, dual donor organic dye for dye-sensitized solar cells. *The Journal of Physical Chemistry C*. 2017;**121**(16):8770-8780
- [103] Cheema H, Peddapuram A, Adams RE, McNamara L, Hunt LA, Le N, et al. Molecular engineering of near infrared absorbing thienopyrazine double donor double acceptor organic dyes for dye-sensitized solar cells. *The Journal of Organic Chemistry*. 2017
- [104] Neale NR, Kopidakis N, Van DL, Grätzel M, Frank AJ. Effect of a coadsorbent on the performance of dye-sensitized TiO<sub>2</sub> solar cells: Shielding versus band-edge movement. *The Journal of Physical Chemistry B*. 2005;**109**(49):23183-23189
- [105] Chandiran AK, Zakeeruddin SM, Humphry-Baker R, Nazeeruddin MK, Grätzel M, Sauvage F. Investigation on the interface modification of TiO<sub>2</sub> surfaces by functional co-adsorbents for high-efficiency dye-sensitized solar cells. *Chemphyschem*. 2017;**18**(19):2724-2731
- [106] Li J, Wu W, Yang J, Tang J, Long Y, Hua J. Effect of chenodeoxycholic acid (CDCA) additive on phenothiazine dyes sensitized photovoltaic performance. *Science China: Chemistry*. 2011;**54**(4):699-706
- [107] Zheng L, Cao Q, Wang J, Chai Z, Cai G, Ma Z, et al. Novel D-A- $\pi$ -A-type organic dyes containing a ladderlike dithienocyclopentacarbazole donor for effective dye-sensitized solar cells. *ACS Omega*. 2017;**2**(10):7048-7056
- [108] Li X, Lin H, Zakeeruddin SM, Grätzel M, Li J. Interface modification of dye-sensitized solar cells with pivalic acid to enhance the open-circuit voltage. *Chemistry Letters*. 2009;**38**(4):322-323
- [109] Kwon YS, Song IY, Lim J, Park S-H, Siva A, Park Y-C, et al. Reduced charge recombination by the formation of an interlayer using a novel dendron coadsorbent in solid-state dye-sensitized solar cells. *RSC Advances*. 2012;**2**(8):3467-3472
- [110] Xu J, Wu H, Jia X, Kafafy H, Zou D. Amidoamine dendron-based co-adsorbents: Improved performance in dye-sensitized solar cells. *Journal of Materials Chemistry A*. 2013;**1**(46):14524-14531
- [111] Wang P, Zakeeruddin SM, Humphry-Baker R, Moser JE, Grätzel M. Molecular-scale interface engineering of TiO<sub>2</sub> nanocrystals: Improve the efficiency and stability of dye-sensitized solar cells. *Advanced Materials*. 2003;**15**(24):2101-2104
- [112] Liu Y, Jennings JR, Wang X, Wang Q. Significant performance improvement in dye-sensitized solar cells employing cobalt(iii/ii) tris-bipyridyl redox mediators by co-grafting alkyl phosphonic acids with a ruthenium sensitizer. *Physical Chemistry Chemical Physics*. 2013;**15**(17):6170-6174
- [113] Liu Y, Jennings JR, Huang Y, Wang Q, Zakeeruddin SM, Grätzel M. Cobalt redox mediators for ruthenium-based dye-sensitized solar cells: A combined impedance spectroscopy and near-IR transmittance study. *The Journal of Physical Chemistry C*. 2011;**115**(38):18847-18855

- [114] Wu K-L, Huckaba AJ, Clifford JN, Yang Y-W, Yella A, Palomares E, et al. Molecularly engineered Ru(II) sensitizers compatible with cobalt(II/III) redox mediators for dye-sensitized solar cells. *Inorganic Chemistry*. 2016;**55**(15):7388-7395
- [115] Omata K, Kuwahara S, Katayama K, Qing S, Toyoda T, Lee K-M, et al. The cause for the low efficiency of dye sensitized solar cells with a combination of ruthenium dyes and cobalt redox. *Physical Chemistry Chemical Physics*. 2015;**17**(15):10170-10175
- [116] Wang M, Li X, Lin H, Pechy P, Zakeeruddin SM, Gratzel M. Passivation of nanocrystalline TiO<sub>2</sub> junctions by surface adsorbed phosphinate amphiphiles enhances the photovoltaic performance of dye sensitized solar cells. *Dalton Transactions*. 2009;(45):10015-10020
- [117] Shen H, Li X, Li J, Wang W, Lin H. Effect of proton numbers of phosphate-based co-adsorbents on the photovoltaic performance of dye-sensitized solar cells. *Electrochimica Acta*. 2013;**97**(Supplement C):160-166
- [118] Zhang Z, Zakeeruddin SM, O'Regan BC, Humphry-Baker R, Grätzel M. Influence of 4-guanidinobutyric acid as coadsorbent in reducing recombination in dye-sensitized solar cells. *The Journal of Physical Chemistry B*. 2005;**109**(46):21818-21824
- [119] Song BJ, Song HM, Choi IT, Kim SK, Seo KD, Kang MS, et al. A desirable hole-conducting coadsorbent for highly efficient dye-sensitized solar cells through an organic redox cascade strategy. *Chemistry - A European Journal*. 2011;**17**(40):11115-11121
- [120] Choi IT, Ju MJ, Kang SH, Kang MS, You BS, Hong JY, et al. Structural effect of carbazole-based coadsorbents on the photovoltaic performance of organic dye-sensitized solar cells. *Journal of Materials Chemistry A*. 2013;**1**(32):9114-9121
- [121] Zhang S, Islam A, Yang X, Qin C, Zhang K, Numata Y, et al. Improvement of spectral response by co-sensitizers for high efficiency dye-sensitized solar cells. *Journal of Materials Chemistry A*. 2013;**1**(15):4812-4819
- [122] Luo J, Wan Z, Jia C, Wang Y, Wu X. A co-sensitized approach to efficiently fill the absorption valley, avoid dye aggregation and reduce the charge recombination. *Electrochimica Acta*. 2016;**215**:506-514
- [123] Aung SH, Hao Y, Oo TZ, Boschloo G. 2-(4-butoxyphenyl)-N-hydroxyacetamide: An efficient preadsorber for dye-sensitized solar cells. *ACS Omega*. 2017;**2**(5):1820-1825
- [124] Yum JH, Holcombe TW, Kim Y, Yoon J, Rakstys K, Nazeeruddin MK, et al. Towards high-performance DPP-based sensitizers for DSC applications. *Chemical Communications*. 2012;**48**:10727-10729
- [125] Pei K, Wu Y, Li H, Geng Z, Tian H, Zhu WH. Cosensitization of D-A- $\pi$ -A quinoxaline organic dye: Efficiently filling the absorption valley with high photovoltaic efficiency. *ACS Applied Materials & Interfaces*. 2015;**7**(9):5296-5304
- [126] Babu DD, Elsherbiny D, Cheema H, El-Shafei A, Adhikari AV. Highly efficient panchromatic dye-sensitized solar cells: Synergistic interaction of ruthenium sensitizer with

- novel co-sensitizers carrying different acceptor units. *Dyes and Pigments*. 2016;**132**:316-328
- [127] Kakiage K, Aoyama Y, Yano T, Otsuka T, Kyomen T, Unno M, et al. An achievement of over 12 percent efficiency in an organic dye-sensitized solar cell. *Chemical Communications*. 2014;**50**(48):6379-6381
- [128] Kakiage K, Aoyama Y, Yano T, Oya K, Kyomen T, Hanaya M. Fabrication of a high-performance dye-sensitized solar cell with 12.8% conversion efficiency using organic silyl-anchor dyes. *Chemical Communications*. 2015;**51**(29):6315-6317
- [129] Cao Y, Cai N, Wang Y, Li R, Yuan Y, Wang P. Modulating the assembly of organic dye molecules on titania nanocrystals via alkyl chain elongation for efficient mesoscopic cobalt solar cells. *Physical Chemistry Chemical Physics*. 2012;**14**(23):8282-8286
- [130] Zhang M, Zhang J, Fan Y, Yang L, Wang Y, Li R, et al. Judicious selection of a pinhole defect filler to generally enhance the performance of organic dye-sensitized solar cells. *Energy & Environmental Science*. 2013;**6**(10):2939-2943
- [131] Kroeze JE, Hirata N, Koops S, Nazeeruddin MK, Schmidt-Mende L, Grätzel M, et al. Alkyl chain barriers for kinetic optimization in dye-sensitized solar cells. *Journal of the American Chemical Society*. 2006;**128**(50):16376-16383
- [132] Lee Y-G, Park S, Cho W, Son T, Sudhagar P, Jung JH, et al. Effective passivation of nanostructured TiO<sub>2</sub> interfaces with PEG-based oligomeric coadsorbents to improve the performance of dye-sensitized solar cells. *The Journal of Physical Chemistry C*. 2012;**116**(11):6770-6777
- [133] Unno M, Kakiage K, Yamamura M, Kogure T, Kyomen T, Hanaya M. Silanol dyes for solar cells: higher efficiency and significant durability. *Applied Organometallic Chemistry*. 2010;**24**(3):247-250
- [134] Sobuś J, Gierczyk B, Burdziński G, Jancelewicz M, Polanski E, Hagfeldt A, et al. Factors affecting the performance of champion silyl-anchor carbazole dye revealed in the femto-second to second studies of complete ADEKA-1 sensitized solar cells. *Chemistry - A European Journal*. 2016;**22**(44):15807-15818
- [135] Gregg BA, Fo P, Ferrere S, Fields CL. Interfacial recombination processes in dye-sensitized solar cells and methods to passivate the interfaces. *The Journal of Physical Chemistry B*. 2001;**105**(7):1422-1429
- [136] Feldt SM, Cappel UB, Johansson EMJ, Boschloo G, Hagfeldt A. Characterization of surface passivation by poly(methylsiloxane) for dye-sensitized solar cells employing the ferrocene redox couple. *The Journal of Physical Chemistry C*. 2010;**114**(23):10551-10558
- [137] Spivack J, Siclován O, Gasaway S, Williams E, Yakimov A, Gui J. Improved efficiency of dye sensitized solar cells by treatment of the dyed titania electrode with alkyl(trialkoxo) silanes. *Solar Energy Materials & Solar Cells*. 2006;**90**(9):1296-1307



- [138] Morris AJ, Meyer GJ. TiO<sub>2</sub> surface functionalization to control the density of states. *The Journal of Physical Chemistry C*. 2008;**112**(46):18224-18231
- [139] Geng Y, Wei Q, Hashimoto K, Tajima K. Dipole layer formation by surface segregation of regioregular poly(3-alkylthiophene) with alternating alkyl/semifluoroalkyl side chains. *Chemistry of Materials*. 2011;**23**(18):4257-4263
- [140] Tada A, Geng Y, Wei Q, Hashimoto K, Tajima K. Tailoring organic heterojunction interfaces in bilayer polymer photovoltaic devices. *Nature Materials*. 2011;**10**:450
- [141] Ma J, Hashimoto K, Koganezawa T, Tajima K. End-on orientation of semiconducting polymers in thin films induced by surface segregation of fluoroalkyl chains. *Journal of the American Chemical Society*. 2013;**135**(26):9644-9647
- [142] Carli S, Casarin L, Caramori S, Boaretto R, Busatto E, Argazzi R, et al. A viable surface passivation approach to improve efficiency in cobalt based dye sensitized solar cells. *Polyhedron*. 2014;**82**:173-180
- [143] Sewvandi GA, Tao Z, Kusunose T, Tanaka Y, Nakanishi S, Feng Q. Modification of TiO<sub>2</sub> electrode with organic silane interposed layer for high-performance of dye-sensitized solar cells. *ACS Applied Materials & Interfaces*. 2014;**6**(8):5818-5826
- [144] Wooh S, Kim T-Y, Song D, Lee Y-G, Lee TK, Bergmann VW, et al. Surface modification of TiO<sub>2</sub> photoanodes with fluorinated self-assembled monolayers for highly efficient dye-sensitized solar cells. *ACS Applied Materials & Interfaces*. 2015;**7**(46):25741-25747
- [145] Matsui M, Mizutani T, Manseki K, Kubota Y, Kubo S, Tomoda H, et al. Effects of alkyl-, polyfluoroalkyl-, and perfluoroalkyl carboxylic acids on the performance of D205 in dye-sensitized solar cells. *Journal of Photochemistry and Photobiology, A: Chemistry*. 2017;**348**(Supplement C):134-138
- [146] Jennings JR, Wang Q. Influence of lithium ion concentration on Electron injection, transport, and recombination in dye-sensitized solar cells. *The Journal of Physical Chemistry C*. 2010;**114**(3):1715-1724
- [147] Konstantakou M, Falaras P, Stergiopoulos T. Blocking recombination in Ru(II) complex-sensitized solar cells by incorporating co-adsorbents as additives in the Co(II)/(III)-based redox electrolytes. *Polyhedron*. 2014;**82**:109-115
- [148] Zhang J, Zaban A. Efficiency enhancement in dye-sensitized solar cells by in situ passivation of the sensitized nanoporous electrode with Li<sub>2</sub>CO<sub>3</sub>. *Electrochimica Acta*. 2008;**53**(18):5670-5674
- [149] Kopidakis N, Neale NR, Frank AJ. Effect of an adsorbent on recombination and band-edge movement in dye-sensitized TiO<sub>2</sub> solar cells: Evidence for surface passivation. *The Journal of Physical Chemistry B*. 2006;**110**(25):12485-12489
- [150] Nath NCD, Jun Y, Lee J-J. Guanidine nitrate (GuNO<sub>3</sub>) as an efficient additive in the electrolyte of dye-sensitized solar cells. *Electrochimica Acta*. 2016;**201**(Supplement C): 151-157



- [151] Afrooz M, Dehghani H. Significant improvement of photocurrent in dye-sensitized solar cells by incorporation thiophene into electrolyte as an inexpensive and efficient additive. *Organic Electronics*. 2016;**29**:57-65
- [152] Boschloo G, Häggman L, Hagfeldt A. Quantification of the effect of 4-tert-butylpyridine addition to I-/I<sub>3</sub><sup>-</sup> redox electrolytes in dye-sensitized nanostructured TiO<sub>2</sub> solar cells. *The Journal of Physical Chemistry B*. 2006;**110**(26):13144-13150
- [153] Nakade S, Kanzaki T, Kubo W, Kitamura T, Wada Y, Yanagida S. Role of electrolytes on charge recombination in dye-sensitized TiO<sub>2</sub> solar cell (1): The case of solar cells using the I-/I<sub>3</sub><sup>-</sup> redox couple. *The Journal of Physical Chemistry B*. 2005;**109**(8):3480-3487
- [154] Kusama H, Arakawa H. Influence of alkylaminopyridine additives in electrolytes on dye-sensitized solar cell performance. *Solar Energy Materials & Solar Cells*. 2004;**81**(1): 87-99
- [155] Sun Z, Zhang R-K, Xie H-H, Wang H, Liang M, Xue S. Nonideal charge recombination and conduction band edge shifts in dye-sensitized solar cells based on adsorbent doped poly(ethylene oxide) electrolytes. *The Journal of Physical Chemistry C*. 2013;**117**(9):4364-4373
- [156] Koh TM, Li H, Nonomura K, Mathews N, Hagfeldt A, Gratzel M, et al. Photovoltage enhancement from cyanobiphenyl liquid crystals and 4-tert-butylpyridine in co(ii/iii) mediated dye-sensitized solar cells. *Chemical Communications*. 2013;**49**(80):9101-9103
- [157] Kakiage K, Tsukahara T, Kyomen T, Unno M, Hanaya M. Significant improvement of photovoltaic performance of dye-sensitized solar cells by using 4-Trimethylsilylpyridine as organic additive to electrolyte solution. *Chemistry Letters*. 2012;**41**(9):895-896
- [158] Hao Y, Yang W, Zhang L, Jiang R, Mijangos E, Saygili Y, et al. A small electron donor in cobalt complex electrolyte significantly improves efficiency in dye-sensitized solar cells. *Nature Communications*. 2016;**7**:13934
- [159] Sun X, Li Y, Mao H, Dou J, Wei M. Towards a high open-circuit voltage by co-additives in electrolyte for high-efficiency dye-sensitized solar cells. *Journal of Power Sources*. 2017;**359**:142-146
- [160] Boschloo G, Hagfeldt A. Characteristics of the iodide/Triiodide redox mediator in dye-sensitized solar cells. *Accounts of Chemical Research*. 2009;**42**(11):1819-1826
- [161] Cong J, Yang X, Kloo L, Sun L. Iodine/iodide-free redox shuttles for liquid electrolyte-based dye-sensitized solar cells. *Energy & Environmental Science*. 2012;**5**(11):9180-9194
- [162] Wu J, Lan Z, Lin J, Huang M, Huang Y, Fan L, et al. Electrolytes in dye-sensitized solar cells. *Chemical Reviews*. 2015;**115**(5):2136-2173
- [163] Saygili Y, Söderberg M, Pellet N, Giordano F, Cao Y, Muñoz-García AB, et al. Copper Bipyridyl Redox Mediators for Dye-Sensitized Solar Cells with High Photovoltage. *Journal of the American Chemical Society*. 2016;**138**(45):15087-15096

- [164] Kusama H, Arakawa H. Influence of benzimidazole additives in electrolytic solution on dye-sensitized solar cell performance. *Journal of Photochemistry and Photobiology, A: Chemistry*. 2004;**162**(2–3):441-448
- [165] Kusama H, Arakawa H. Influence of pyrimidine additives in electrolytic solution on dye-sensitized solar cell performance. *Journal of Photochemistry and Photobiology, A: Chemistry*. 2003;**160**(3):171-179
- [166] Kusama H, Arakawa H. Influence of quinoline derivatives in I<sup>–</sup>/I<sub>3</sub><sup>–</sup> redox electrolyte solution on the performance of Ru(II)-dye-sensitized nanocrystalline TiO<sub>2</sub> solar cell. *Journal of Photochemistry and Photobiology, A: Chemistry*. 2004;**165**(1–3):157-163
- [167] Yin X, Tan W, Zhang J, Lin Y, Xiao X, Zhou X, et al. Synthesis of pyridine derivatives and their influence as additives on the photocurrent of dye-sensitized solar cells. *Journal of Applied Electrochemistry*. 2009;**39**(1):147-154
- [168] Gao J, Yang W, Pazoki M, Boschloo G, Kloo L. Cation-dependent photostability of Co(II/III)-mediated dye-sensitized solar cells. *The Journal of Physical Chemistry C*. 2015; **119**(44):24704-24713
- [169] Gao J, Bhagavathi Achari M, Kloo L. Long-term stability for cobalt-based dye-sensitized solar cells obtained by electrolyte optimization. *Chemical Communications*. 2014;**50**(47): 6249-6251
- [170] Suzuki K, Yamaguchi M, Kumagai M, Tanabe N, Yanagida S. Dye-sensitized solar cells with ionic gel electrolytes prepared from imidazolium salts and agarose. *Comptes Rendus Chimie*. 2006;**9**(5):611-616
- [171] Ileperuma O. Gel polymer electrolytes for dye sensitised solar cells: A review. *Materials Technology*. 2013;**28**(1–2):65-70
- [172] De Gregorio GL, Agosta R, Giannuzzi R, Martina F, De Marco L, Manca M, et al. Highly stable gel electrolytes for dye solar cells based on chemically engineered polymethacrylic hosts. *Chemical Communications*. 2012;**48**(25):3109-3111

IntechOpen